PREPARATION AND CHARACTERIZATION OF STARCH FILMS REINFORCED WITH CITRATE
CELLULOSE NANOCRYSTALS

Miss Prapaporn Nakarat

A Thesis Submitted in Partial Fulfillment of the Requirements
for the Degree of Master of Science in Petrochemistry and Polymer Science
Field of Study of Petrochemistry and Polymer Science
Faculty of Science
Chulalongkorn University
Academic Year 2018
Copyright of Chulalongkorn University

การเตรียมและการพิสูจน์เอกลักษณ์ของฟิล์มแป้งเสริมแรงด้วยซิเทรตเซลลูโลสนาโนคริสตัล

น.ส.ประภาพร นาคราช

Thesis Title	PREPARATION AND CHARACTERIZATION OF STARCH FILMS REINFORCED WITH CITRATE CELLULOSE NANOCRYSTALS
By	Miss Prapaporn Nakarat
Field of Study	Petrochemistry and Polymer Science
Thesis Advisor	Assistant Professor Pattara Thiraphibundet, Ph.D.

Accepted by the Faculty of Science, Chulalongkorn University in Partial Fulfillment of the Requirement for the Master of Science

.... Dean of the Faculty of Science

(Professor Polkit Sangvanich, Ph.D.)

THESIS COMMITTEE

.... Chairman

(Assistant Professor Warinthorn Chavasiri, Ph.D.)

.... Thesis Advisor

(Assistant Professor Pattara Thiraphibundet, Ph.D.)

.... Examiner

(Associate Professor Sirilux Poompradub, Ph.D.)

.... External Examiner

(Assistant Professor Karnthidaporn Wattanakul, Ph.D.)

ประภาพร นาคราช : การเตรียมและการพิสูจน์เอกลักษณ์ของฟิล์มแป้งเสริมแรงด้วยซิเทรตเซลลูโลสนาโนคริสตัล. (
PREPARATION AND CHARACTERIZATION OF STARCH FILMS REINFORCED WITH CITRATE CELLULOSE NANOCRYSTALS) อ.ที่ปรึกษาหลัก : ผศ. ดร.พัฒทรา ธีรพิบูลย์เดช

แบคทีเรียลเซลลูโลสนาโนคริสตัลที่ปรับปรุงด้วยซิเทรต (ซิเทรตเซลลูโลสนาโนคริสตัล) ถูกเตรียมขึ้นด้วยวิธีการใช้กรดสองชนิดภายในขั้นตอนเดียว (กรดซิตริกและกรดไฮโดรคลอริก) และนำมาเสริมแรงในฟิล์มแป้งสามชนิด ได้แก่ แป้งข้าวโพด แป้งข้าวสาลีและแป้งข้าวจ้าว ความยาวและความกว้างเฉลี่ยของซิเทรตเซลลูโลสนาโนคริสตัลเท่ากับ 583 และ 46 นาโนเมตร ตามลำดับ ระดับการแทนที่ของหมู่ฟังก์ชันคือ 0.075 และค่าดัชนีความเป็นผลึกของซิเทรตเซลลูโลสนาโนคริสตัลใกล้เคียงกับแบคทีเรียลเซลลูโลสเดิม ได้ศึกษาปริมาณของซิเทรตเซลลูโลสนาโนคริสตัล (0-20เปอร์เซ็นต์โดยน้ำหนักของแป้ง)ที่มีผลต่อสมบัติของฟิล์ม ฟิล์มแป้ง 3 ชนิดให้ของผลการทดลองในแนวโน้มเดียวกัน ความหนาของฟิล์มส่วนใหญ่อยู่ในช่วง 0.20-0.24 มิลลิเมตรและเมื่อเพิ่มปริมาณซิเทรตเซลลูโลสนาโนคริสตัลมีผลทำให้ฟิล์มมีความขุ่นเพิ่มขึ้น จากภาพถ่ายลักษณะทางสัณฐานวิทยาด้วยเทคนิค FE-SEM แสดงให้เห็นว่าซิเทรตเซลลูโลสนาโนคริสตัลกระจายตัวได้ดีในเมทริกซ์ของฟิล์มแป้ง การเพิ่มซิเทรตเซลลูโลสนาโนคริสตัลในแป้งทั้งสามชนิดแสดงให้เห็นถึงการเพิ่มขึ้นของดัชนีค่าความเป็นผลึก อุณหภูมิการสลายตัวและสมบัติเชิงกล นอกจากนี้ความต้านทานแรงดึงของฟิล์มแป้ง/ซิเทรตเซลลูโลสนาโนคริสตัลเพิ่มขึ้นเป็นลำดับ ในขณะที่ค่ายังโมดุลัสเพิ่มขึ้นอย่างรวดเร็ว ซึ่งแสดงให้เห็นว่าความยืดหยุ่นของฟิล์มลดลงเมื่อปริมาณซิเทรตเซลลูโลสนาโนคริสตัลเพิ่มขึ้น ในแป้งสามชนิดนี้พบว่าซิเทรตเซลลูโลสนาโนคริสตัลมีอิทธิพลสูงสุดต่อสมบัติเชิงกลของแป้งข้าวสาลี

สาขาวิชา   ปิโตรเคมีและวิทยาศาสตร์พอลิเมอร์   ลายมือชื่อนิสิต ....

ปีการศึกษา 2561   ลายมือชื่อ อ.ที่ปรึกษาหลัก ....

5872141823 : MAJOR PETROCHEMISTRY AND POLYMER SCIENCE

KEYWORD: citrate CNCs, corn starch film, wheat starch film, rice starch film

Prapaporn   Nakarat   : PREPARATION AND CHARACTERIZATION OF STARCH FILMS REINFORCED WITH CITRATE CELLULOSE NANOCRYSTALS. Advisor: Asst. Prof. Pattara Thiraphibundet, Ph.D.

Citrate-modified bacterial cellulose nanocrystals (citrate CNCs) were prepared by a green one-pot dual acid (citric and hydrochloric acids) method and used them to reinforce three types of starch films; corn, wheat and rice starch films. The average length and width of citrate CNCs were 583 and 46 nm, respectively. The degree of citrate substitution on CNCs was 0.075 and its crystallinity index was closely to the original bacterial cellulose. The effect of various amount of citrate CNCs (0-20%wt of starch) on film property was study. Three starch films showed the same trend of examination results. The film thickness of most films was in a range of 0.20-0.24 mm and the increase of CNCs amount increase the film turbidity. The FE-SEM morphology revealed the good dispersion of citrate CNCs in the starch film matrix. The addition of citrate CNCs in all starches showed the continuing enhancement of crystallinity, T_{deg}, and mechanical property. The tensile strength of starch/citrate CNCs films increased gradually while Young's modulus increased dramatically. This indicated that the elasticity of films decreased if the amount of citrate CNCs increased. Among of three starches, citrate CNCs exhibited the highest influence on the mechanical property of wheat starch films.

Field of Study: Petrochemistry and Polymer Science

Academic Year: 2018

Student's Signature ....

Advisor's Signature ....

ACKNOWLEDGEMENTS

จุฬาลงกรณ์มหาวิทยาลัย
CHULALONGKORN UNIVERSITY

TABLE OF CONTENTS

Page

LIST OF FIGURES

LIST OF TABLES

LIST OF ABBREVIATIONS

et al.	et alli, and other
%	percentage
β	beta position
$°C$	degree celsius
cm^{-1}	unit of wavenumber (IR)
Fig	figure
ATR-FTIR	attenuated total reflection fourier transform infrared
wt	weight
mL	milliliter
min	minute
nm	nanometer
rpm	revolution per minute
h	hour
FE-SEM	field emission scanning electron microscopy
kV	kilovolt
TGA	thermogravimetric analysis
DSC	differential scanning calorimetry
mm	millimeter
TG	thermogravimetric
DTG	thermogravimetric derivative

CHAPTER I

INTRODUCTION

1.1 Motivation of research

In recent times, scientific community has been focusing on the replacement of petroleum-based polymers by others more environmentally friendly such as agricultural resources. Plastic waste is a rising environmental problem because of the difficulty of their disposal. Starch is one of the promising sources for producing biodegradable plastics. Starch granules differ in shape, size, structure and chemical composition, depending on the origin of the starch [1]. They are considered as semi-crystalline and composed of amylose and amylopectin. Amylose is a linear polysaccharide of α-1,4 anhydroglucose units whereas amylopectin is a highly branched polymer of short α-1,4 chains linked by α-1,6 glucosidic branching points occurring every 25–30 glucose units [2]. Amylose and amylopectin ratio has a great impact on the physical and chemical properties of starch. High contents of amylose produce more rigid films while amylopectin branches are mainly responsible for the material crystallinity and producing less rigid films [3]. However, the starch films are brittle and poor mechanical properties [4]. Many studies have reported the reinforcing fillers for improving their properties such as kaolin [5], taro starch nanoparticles [6], multi-walled carbon nanotubes [7], lignin [8], cellulose fiber [9], and cellulose nanocrystals (CNCs) [10]. The sources of cellulose are mainly derived from plants [11] and bacterial [12]. Bacterial cellulose (BC) has unique feature which is its high purity without the presence of hemicellulose and lignin in which different from plant cellulose. Moreover, BC has high crystallinity, biocompatible, high surface area and superior mechanical properties [13]. BC is generally produced from a strain of Acetobacter xylinum. And the incorporation of BC in several of polymer matrices such as starch [14], poly (lactic acid) (PLA) [15], poly (vinyl alcohol) (PVA) [16], natural rubber (NR) [17] and polyurethane (PU) [18] had been reported. CNCs have attracted a great deal of interest in the nanocomposite field due to their appealing intrinsic properties such as nanoscale dimensions, high surface area, low density, renewability,

biodegradability and high mechanical strength. CNCs have a high aspect ratio and thus provide better reinforcing effects. For example, the outstanding improvement of tensile strength and modulus of pea starch was observed when 30 wt% CNCs was introduced [10]. Comparing to the neat pea starch film, the tensile strength and Young's modulus of film with 30 wt % CNCs were enhanced by 305% and 1,561%, respectively. CNCs are obtained from acid hydrolysis of cellulose.

However, the strong hydrogen bonds between adjacent CNCs cause the CNC-aggregation in the film matrix. There are some studies reported that introducing the carboxyl group on CNCs can enhance the aqueous dispersion of CNCs [19-21]. Recently, the one-pot procedure combining both cellulose acid-catalyze hydrolysis and surface-modification to prepare malonate, malate and citrate CNCs was reported [19]. All modified CNCs showed the stable aqueous colloidal suspensions with no sedimentation after 7 days. And the incorporation of citrate CNCs in the polyvinyl alcohol nanocomposite was found to exhibit the highest thermal stability.

Based on our knowledge, the addition of the citrate CNCs in the starch-based films has not been reported. Thus, the main objective of this study was to investigate the influence of citrate CNCs as reinforcing agent for three types of starch: corn, wheat and rice starches. Citrate CNCs were prepared from BC by a green one-pot procedure which included both cellulose acid-catalyzed hydrolysis and surface-modification. This reaction is carried out in an acid mixture composed of hydrochloric and citric acid. Then, starch films reinforced with different amount of citrate CNCs were prepared by a casting method. The morphology and thermal property of the films were investigated by field emission scanning electron microscopy (FE-SEM), Fourier transform infrared (FTIR) spectroscopy, X-ray diffraction (XRD), thermogravimetric analysis (TGA), differential scanning calorimetry (DSC). In addition, the mechanical property, transparency, contact angle and water uptake of films were also studied.

CHAPTER II

THEORY AND LITERATURE REVIEWS

In this work, starch films reinforced with different amounts of citrate CNCs were prepared by a casting method. Three types of starch: corn, wheat and rice starches were studied. Citrate CNCs were prepared by a green one-pot procedure which included both bacterial cellulose acid-catalyzed hydrolysis and surface-modification. This reaction is carried out in an acid mixture composed of hydrochloric and citric acid. The hydrolysis of amorphous cellulose segments can be performed simultaneously with the esterification of accessible hydroxyl groups to be carboxyl group. We expected that citrate CNCs as reinforce agent improved the mechanical properties of those starch films. The following theory and literature reviews were involved in this research.

2.1 Bacterial cellulose (BC)

2.1.1 Source and general properties

Bacterial cellulose (BC) is obtained from *nata-de-coco* (Fig. 2.1(a)), a South-East Asian food product. BC generally produce by the gram negative bacteria *Acetobacter xylinum* (or *Gluconacetobacter xylinum*), which manifests itself under special culturing conditions as a fine fibrous network of fibers (Fig. 2.1(b)) [13]. BC is three-dimensional nanoporous fiber networks with fiber diameters of approximately 30–50 nm, much thinner than plant cellulose [22]. The β-1,4-D-glucan chains (Fig. 2.1(c)) in BC associates strongly via hydrogen bonding and are responsible for the high degree of crystallinity (up to 90%) and good mechanical stability of cellulose [23, 24]. Young's modulus and tensile strength of BC are about 15–35 GPa and 200–300 MPa, respectively [25, 26]. Moreover, BC has high purity without the presence of hemicellulose and lignin. Its simple production and purification process makes BC attractive. BC is widely used in food industry as *nata-de-coco* in sugar syrup for desserts and fruit cocktails. Apart from this application, BC is used in several applications such as scaffold for tissue engineering [27], wound healing [28], acoustic

diaphragms [29], ion exchange membranes [30], electronic devices [31], and reinforcement for many materials.

| (a) | (b) | (c) |
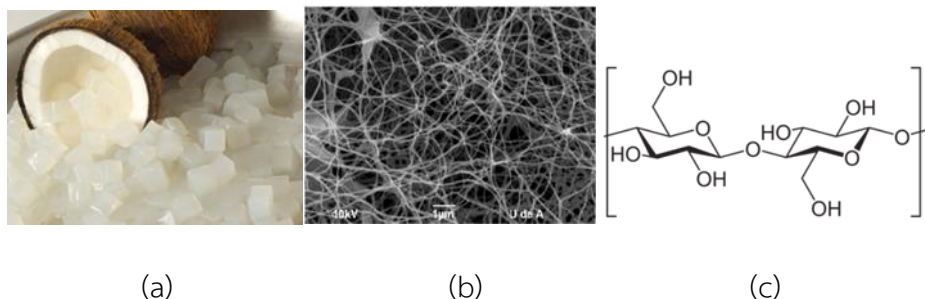
Figure 2.1 (a) nata-de-coco, (b) bacterial cellulose fiber and (c) bacterial cellulose structure.

However, in this study we interested BC to use as a reinforcing agent. The following studies were some reports about materials reinforced by BC.

In 2009, Wan and colleagues [14] prepared the BC nanofiber–starch biocomposites manufactured by solution impregnation method. The increase of fiber content from 7.8-22.0 wt% increased the tensile strength and Young's modulus for 2.03-2.37 times comparing to the pure starch and 111-132%, respectively. However, a decrease in elongation at break was observed if the fiber content increased. In addition, the presence of BC nanofibers improved the resistance to moisture and microorganism attack.

In 2010, Eliane and colleagues [32] fabricated composite materials from the water-based suspensions of the acrylic emulsions and BC nanofibrils. The composite material with 10% of BC showed the rise of around 30 $^\circ$C in the maximum degradation temperature. The tensile tests revealed that increasing bacterial cellulose load affected the substantial increase in Young's modulus and tensile strength, but a corresponding decrease in elongation at break.

In 2015, Sirilak and colleagues [33] studied reinforcement of natural rubber (NR) with BC *via* latex solution process. There was no aggregation of BC in the NR matrix. The mechanical properties, such as Young's modulus and tensile strength, of NR composite increased by an increased load of BC, while elongation at break was decreased. The maximal Young's modulus and tensile strength at 4910.4 and 98.4 MPa, respectively, were obtained with BC loading at 80%.

BC can be used as a strong reinforcement. Moreover, nanoscale dimensions and modification of the functional group on the BC surface played an important role in better improvement of the mechanical and thermal properties for use in several applications.

2.1.2 Acid hydrolysis and surfaces modification of cellulose

2.1.2.1 Acid hydrolysis

Acid hydrolysis is a common method used for producing cellulose nanocrystals (CNCs) from cellulose fiber. With this approach, hydrogen ions (H^+) of acid penetrate amorphous cellulose molecules promoting cleavage of glycosidic bonds, thus releasing individual crystallites (Fig. 2.2) [34]. The physical properties of nanocrystals such as crystallite size, size distribution and surface characteristics depend on the cellulose source and the hydrolysis reaction conditions (i.e., the acid type and concentration, reaction time and temperature). Sulfuric acid (H_2SO_4) and hydrochloric acid (HCl) are most commonly used for the acid hydrolysis of cellulose. Hydrochloric acid generates low-density surface charges on the CNCs with limited nanocrystal dispersibility, which tends to promote flocculation in aqueous suspensions. In contrast, when sulfuric acid is used, a highly stable colloidal suspension is produced because of the high negative surface charge promoted by sulfonation of the CNCs surface. However, the presence of sulfate groups ($-OSO_3^-$) reduces the thermal stability of the nanocrystals [35].
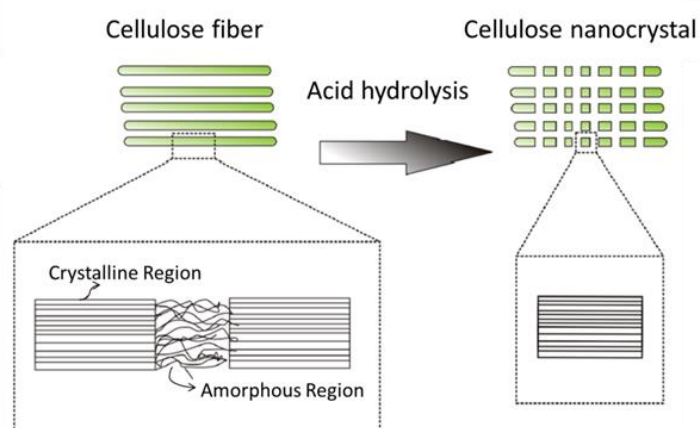
Figure 2.2 Scheme of acid hydrolysis of cellulose [12].

CNCs have attracted a great deal of interest in the nanocomposite field due to their appealing intrinsic properties such as nanoscale dimensions, high surface area, unique morphology, low density, renewability, biodegradability and high mechanical strength. The conversion of cellulose fibers into nanocrystals results in the formation of whiskers with large aspect ratio, mainly due to their nanoscale dimensions. This superior aspect ratio plays a critical role in their reinforcement potential when used for the fabrication of polymer nanocomposite materials.

In 2008, Cao and colleagues [10] prepared CNCs by acid hydrolysis (H_2SO_4) of flax fiber. Flax cellulose nanocrystals (FCNs) consisted of slender rods with lengths ranging from 100 to 500 nm and diameters ranging from 10 to 30 nm (Fig. 2.3(a)). The plasticized starch (PS) reinforced with FCNs were obtained by the casting method. The FCNs well dispersed within the PS matrix and had good adhesion in the interfacial area. These reasons led to an increase of glass transition temperature of film and the existence of FCNs reduced the flexibility of starch molecular chains. The tensile strength and Young's modulus of the FCNs starch film increased from 3.9 to 11.9 MPa and from 31.9 to 498.2 MPa, respectively, with an increase of FCNs content from 0 to 30 wt%. Meanwhile, this film also showed a higher water resistance.

In 2012, Johnsy and colleagues [36] fabricated gelatin based edible nanocomposite films by incorporating bacterial CNCs at various concentrations ranging from 1 to 5 wt%. CNCs were obtained by acid hydrolysis (HCl) of edible bacterial cellulose fibers. The formation of rod like cellulose nanocrystals was having an average diameter and length of 20 ± 5 nm and 290 ± 130 nm, respectively (Fig. 2.3(b)). The formation of percolated networks of CNCs within gelatin matrix resulted in improving the mechanical properties of nanocomposites. Highly crystalline CNCs reduced the moisture sorption and moisture barrier properties of gelatin by interacting with hydrophilic sites of gelatin and reducing its effectiveness in moisture uptake. The addition of bacterial CNCs had also affected the segmental mobility of gelatin chains, which in turn resulted in an increased glass transition temperature. High thermal stability of cellulose nanocrystals also contributed the improvement of the degradation temperature and the dynamic mechanical properties of gelatin.

In 2014, Guangping and colleagues [37] prepared CNCs from microcrystalline cellulose by acid hydrolysis (H_2SO_4). The average length and width of homogenized CNCs were 152±30 and 10±3 nm, respectively (Fig. 2.3(c)). CNCs-reinforced polymethylmethacrylate (PMMA) composite films at various CNCs loadings (0-20 wt%) were made using solution casting methods. The addition of CNCs in the PMMA matrix decreased the optical transparency of the nanocomposites. The light transmittance at 600 nm wavelengths was limited at 4.9% when 20 wt% CNCs content was used. The tensile properties were enhanced with increasing CNCs content in the PMMA matrix. CNCs contributed the improvement of Young's modulus more than that of tensile strength.
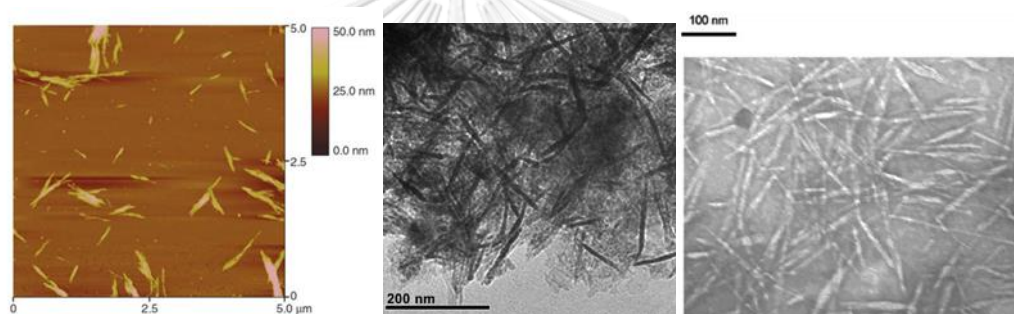
Figure 2.3 (a) AFM topography image of FCNs from acid hydrolysis (HCl) [10], (b) TEM images of bacterial CNCs from acid hydrolysis (H_2SO_4) [36] and (c) TEM images of CNCs from acid hydrolysis (H_2SO_4) [37].

2.1.2.2 Surfaces modification

CNCs possess high surface areas with reactive hydroxyl groups which facilitate surface modification in order to fine tune surface topochemistry and extend their applications (Fig. 2.4). Such modifications are critical to enable their dispersion within bioplastic matrices and to create strong fiber-matrix adhesion [19-21]. The modification of CNC surfaces has been extensively explored.
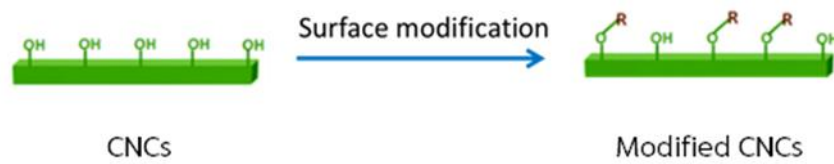
CNCs   Modified CNCs

Figure 2.4 Scheme of surface modification of cellulose nanocrystals [38].

In 2011, Ning Lin and colleagues [38] modified cellulose nanocrystals with acetic anhydride (Fig. 2.5(a)). With the substitution of hydroxyl groups by acetyl groups on the CNC surface, acetylated cellulose nanocrystals (ACN) exhibited a good dispersion in six common solvents, a decrease in surface polarity and a higher decomposition temperature. When the 6 %wt of ACN filler was introduced into the polylactic acid (PLA), the tensile strength of the PLA/ACN-6 nanocomposite was enhanced by 61.3% and the Young's modulus was 1.5-fold greater than those of the neat PLA sheet. This improvement was primarily attributed to uniform dispersion of the ACN and to strong interfacial adhesion between filler and matrix.

In 2015, Ragab and colleagues [39] oxidized CNCs with 2,2,6,6-tetramethyl-1-piperidinyloxyl (TEMPO) (Fig. 2.5(b)). The prepared CNCs-TEMPO was used as reinforcing elements in chitosan nanocomposites. The addition of CNCs or CNCs-TEMPO to chitosan resulted in significant increase of its tensile strength up to 5% of nanocrystals loading, above which a decrease in tensile strength was replace. At lower 5% of nanocrystals content, the incorporation of CNCs-TEMPO in chitosan nanocomposites increased the tensile strength more than that of CNCs. The higher tensile strength of nanocomposites containing CNCs-TEMPO than that containing CNCs could be endorsed the stronger ionic interaction between the negative charges of CNCs-TEMPO and the positive charges of chitosan chains. In addition, chitosan nanocomposites containing CNCs-TEMPO displayed higher rate of dissolution in simulated body fluid (SBF) than those containing CNCs.

In 2018, Ferreira and colleagues [40] modified cellulose nanocrystals (CNCs) with adipic acid. The decrease in hydrophilicity occurred mainly by addition of adipic acid onto the CNC surface after surface modification due to the addition of methylene groups (Fig. 2.5(c)). Thus, unmodified CNCs approach potential

applications as reinforcement in hydrophilic polymeric matrices, while modified CNCs interact better with hydrophobic matrices.

(a)   (b)

(c)
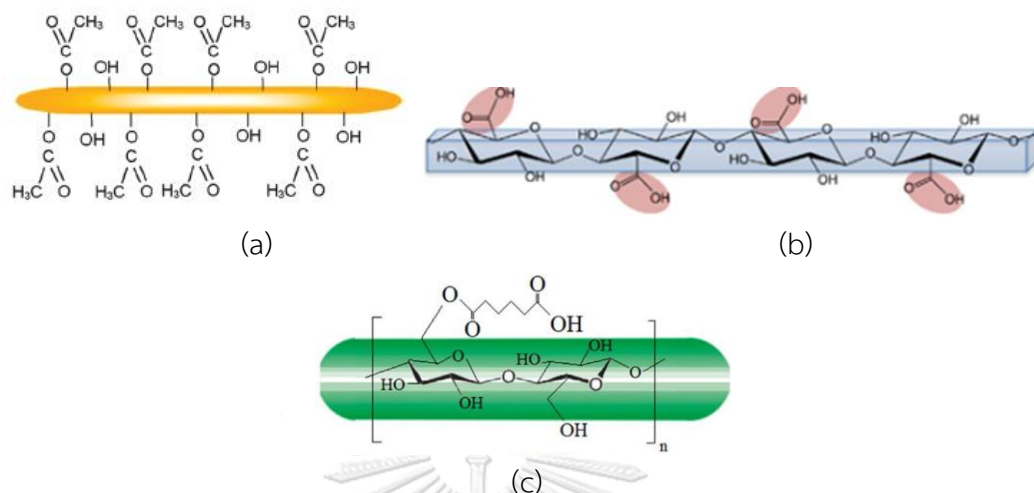
Figure 2.5 (a) acetylated cellulose nanocrystals (ACN) [38], (b) CNCs-TEMPO [39] and (c) surface modification of CNCs with adipic acid [40].

2.1.1.3 Acid hydrolysis and surface-modification by one-pot procedure

Generally, surface modified cellulose nanocrystals (modified-CNCs) from cellulose fiber were performed using multiple reaction steps. Recently, cellulose can be hydrolyzed and modified in a single step by a one-pot procedure. For example, carboxylate CNCs were produced by a combination of concurrent acid hydrolysis of amorphous cellulose chains and organic acid-catalyzed Fischer esterification of accessible hydroxyl groups, resulting in surface-modified CNCs. The organic acid can be chosen for desired functionality, hydrophilicity, or hydrophocity to the modified CNCs. By this method, modifications can be achieved to modulate the surface properties of CNC without the need for tedious and non-practical solvent-exchange protocols [19-21].

In 2008, Birgit and colleagues [20] reported acid hydrolysis and surface-modification by one-pot procedure as efficient method for preparation of acetylated CNCs (Fig. 2.6). The reaction was performed by dispersing cellulose in acetic acid with addition of a catalytic quantity of hydrochloric acid. Resulting CNCs were of similar dimensions compared to those obtained by hydrochloric acid hydrolysis alone. The

acetylated CNCs were dispersible in ethyl acetate and toluene which indicated the increasing of hydrophobicity. Thus, the acetylated CNCs were compatible with hydrophobic polymers and can used as a reinforcing phase.

In 2015, Stephen and colleagues [21] prepared acetate and lactate modified CNCs (AA-CNCs and LA-CNCs) from cotton cellulose by a green one-pot dual acid (HCl and acetic/lactic acid) method (Fig. 2.7). Relative to unmodified CNCs, lactate and acetate moieties on the CNC surfaces increased the thermal stability for 40°C. Polylactide (PLA) nanocomposites reinfored with LA-, AA- and unmodified CNCs were fabricated by direct melt blending. At 5 wt% CNCs loading, LA-CNCs gave the highest storage modulus and matrix dispersion.

Subsequently, malonate, malate and citrate CNCs from ramie cellulose were prepared using bio-based di- and tri-functional organic acids (malonic, malic acid or citric acid) and HCl (Fig. 2.8) [19]. All modified CNCs showed the stable aqueous colloidal suspensions with no sedimentation after 7 days due to free carboxylic acid functionality on CNC surfaces. Nanocomposites of poly(vinyl alcohol) with 1%wt of each modified CNCs were prepared. It was found that the polyvinyl alcohol-citrate-modified CNC nanocomposite exhibited the highest thermal stability.
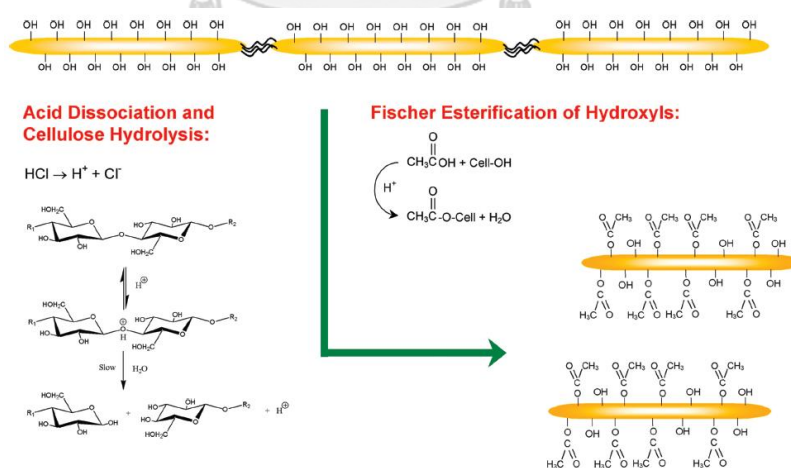
Figure 2.6 Reaction scheme illustrating the simultaneous occurrence of cellulose hydrolysis and esterification of hydroxyl groups is using a mixture of acetic and hydrochloric acid as example [20].
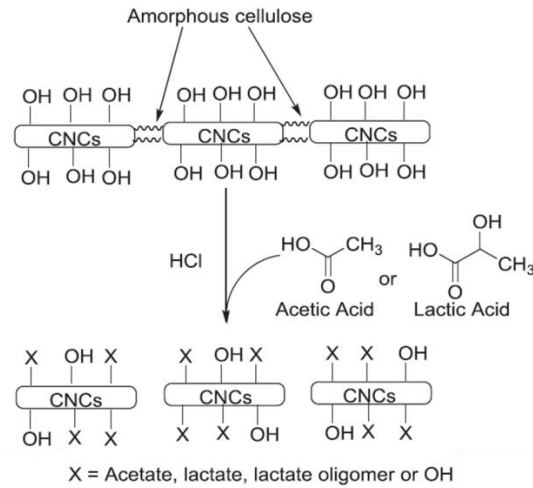
Figure 2.7 Green one-pot hydrolysis/Fischer esterification process to form modified CNCs [21].
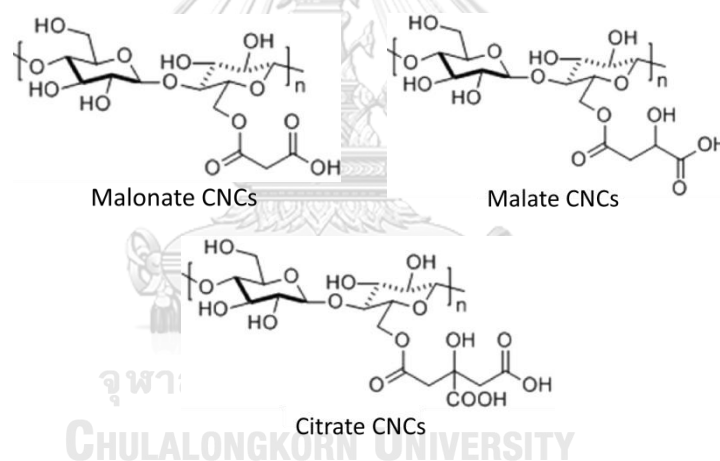
Figure 2.8 Malonate, malate and citrate CNCs [19].

2.2 starch

2.2.1 Source and general properties

Starch is one of the most abundant natural polysaccharide raw materials. It is a renewable resource, low-cost and widely available. Starch granules differ in shape, size, structure, and chemical composition, depending on the origin of the starch [1]. Native starch is composed of two main components that are amylose and amylopectin (Fig. 2.9). Other minor components such as lipids, phospholipids and

phosphate monoester derivatives are also found in starch. Amylose is a linear polymer of α-1,4 anhydroglucose units that has excellent film-forming ability [2]. Meanwhile, amylopectin is a highly branched polymer of short α-1,4 chains linked by α-1,6 glucosidic branching points occurring every 25–30 glucose units [3]. The ratio of amylose and amylopectin depends on the source and age of the starch. General starch will contain 20 to 25 % amylose and 75 to 80 % amylopectin [41]. The starch that has low or no amylose is normally called waxy starch, whereas starch which contains more than 50% of amylose is high-amylose starch.
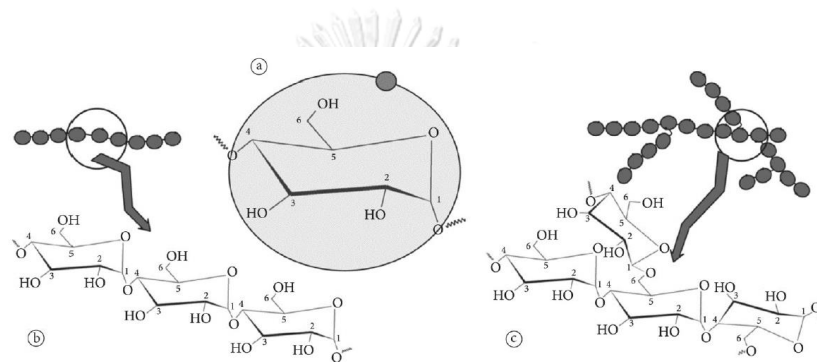
Figure 2.9 Basic structure design of (a) glucose units, (b) amylose and (c) amylopectin [42].

Starch granules are not soluble in cold water due to the fact that strong hydrogen bonds hold the starch chains together. However, when starch molecules are heated in water excess, the semi-crystalline structure is broken, and water molecules associate by hydrogen bonding to hydroxyl groups exposed on the amylose and amylopectin molecules. This association causes swelling and increases granule size and solubility [42]. Heating starch suspensions in an excess of water and at high temperatures (between 65 and 100 °C approximately depending on the type of starch) provokes an irreversible gelatinization process.

Starch is widely used in food industry. Moreover, the starch composite materials as biodegradable polymers have been of a great interest to compensate the uses of non-biodegradable petroleum-based polymers.

2.2.2 Starch-Based Films

Starch is one of the promising sources for producing biodegradable plastics. However, the starch films are mostly water-soluble, brittle and have poor mechanical properties [4]. One way to reduce these drawbacks is the reinforcement of starch films using organic and inorganic fillers to form biocomposites. The following studies were some reports about fabrication of starch films using different reinforcement agents such as kaolin, cellulose fiber, CNCs and modified CNCs.

In 2001, Carvalho and colleagues [5] prepared corn starch plasticized with glycerin and reinforced with hydrated kaolin. The composite with 50 phr kaolin showed an increase of the tensile strength from 5 to 7.5 MPa, the modulus of elasticity from 120 to 290 MPa but exhibited a decreased of the tensile strain at break from 30 to 14%.

In 2011, Amanda and colleagues [9] developed biodegradable films based on rice flour reinforced with cellulose fibers by using casting method (Fig. 2.10). Glycerol and sorbitol were used as plasticizer. Cellulose fiber had the water vapor permeability and tensile strength higher than films without fibers. Moreover, it was found that glycerol is suitable for rice flour due to easier peel off from acrylic Petri dishes than sorbitol.
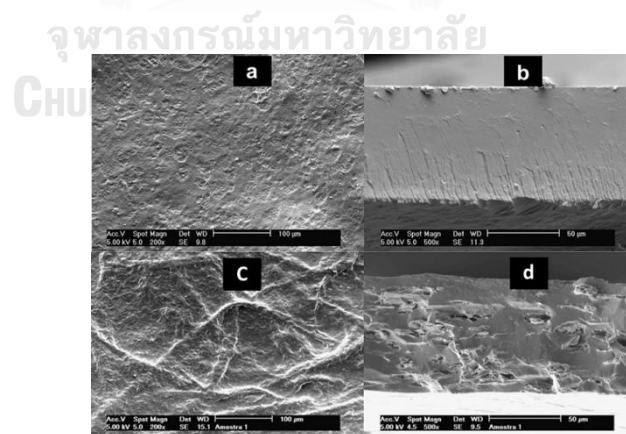

Figure 2.10 SEM Micrographs of films surfaces (left) and fractures (right): (a) and (b) rice flour film plasticized with glycerol; (c) and (d) rice flour-cellulose fiber film plasticized with glycerol.

In 2015, Lei Dai and colleagues [6] used 0.5–15% of taro starch nanoparticles (TSNPs) as reinforcing agents in corn starch films. Glycerol was used as plasticizer. An increase in the content of TSNPs led to a significant decrease in the water vapour permeability of films. The addition of TSNPs increased the tensile strength of films from 1.11 MPa to 2.87 MPa. Compared with native starch films, the surfaces of nanocomposite films became uneven (Fig. 2.11). The onset temperature and melting temperature of films containing TSNPs were higher than those of native starch films. Thus, the addition of TSNPs improved the thermal stability of corn starch films.
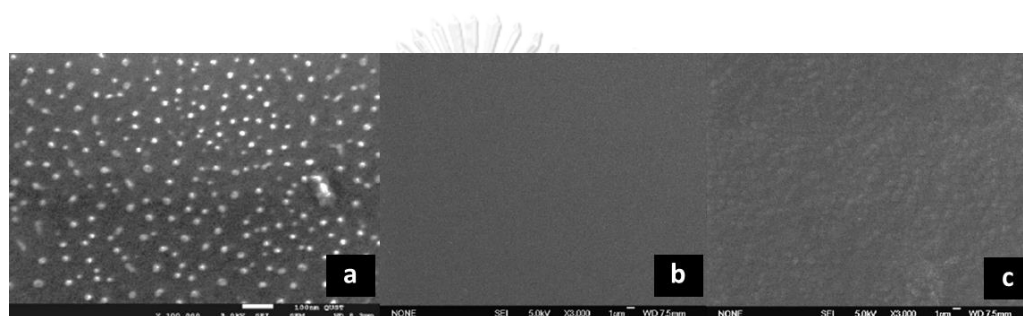
Figure 2.11 SEM images of (a) taro starch nanoparticles (TSNPs), (b) surfaces of native starch films and (c) surfaces of starch films reinforced with 15% of TSNPs.

In 2014, Aníbal and colleagues [43] prepared starch films reinforced with 3% cellulose nanocrystals (CNCs) obtained from sugarcane bagasse. Glycerol was used as plasticizer. The incorporation of CNCs into the starch films improved their water resistance and water barrier properties. The addition of CNCs increased the tensile strength and Young' modulus of films from 2.8 to 17.4 MPa and from 112 to 520 MPa, respectively, comparing to control film. The elongation at break decreases from 44.9 to 9.1% due to the rigid nature of the filler.

In 2017, Xiaohan and colleagues [44] fabricated cassava starch film reinforced with carboxymethyl cellulose nanocrystals (N-CMCs). The N-CMCs/cassava starch films showed better mechanical properties and water solubility comparing to cassava starch film. Moreover, the water vapor permeability and moisture absorption of the N-CMCs/cassava starch film decreased by 42.7% and 15.9%, respectively.

The N-CMCs/cassava starch films had a more cohesive structure and the N-CMCs were well dispersed in the starch matrix (Fig. 2.12).

Figure 2.12 SEM photographs the cross sections of (a) Starch film, (b) CNCs/cassava starch film and (c) N-CMCs/cassava starch film.
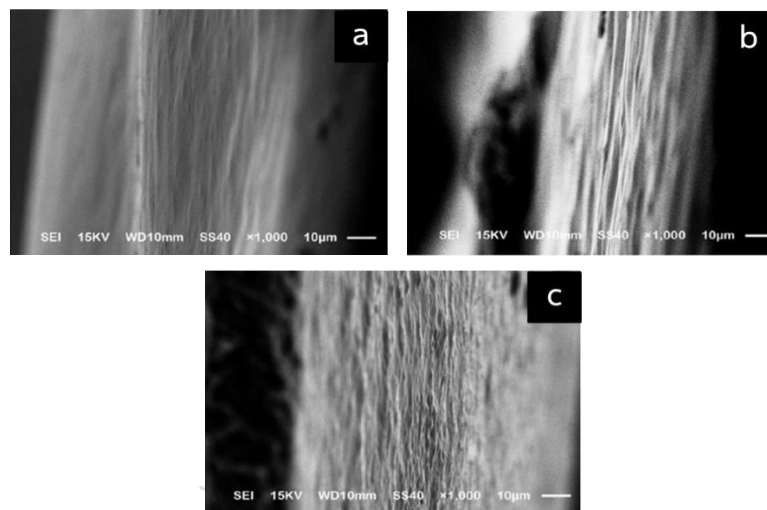
จุฬาลงกรณ์มหาวิทยาลัย

CHULALONGKORN UNIVERSITY

CHAPTER III

EXPERIMENTALS

3.1 Chemicals and Materials

Bacterial cellulose (BC) pellicles were obtained from a local market in Chonburi, Thailand. Citric acid was supplied by CHEMIPAN Company, Thailand. Sodium hydroxide (NaOH) was purchased from Merck (Germany). Hydrochloric (HCl) was ACS reagent grade and purchased from Merck (Germany). Corn starch was purchased from Continental Food Co., LTD. (Thailand). Wheat starch was purchased from Mane Fils Co., Ltd. (Australia). Rice starch was purchased from Thai Flour Industry Co., LTD. (Thailand). Glycerol was AR grade and purchased from QRëC (New Zealand).

3.2 Preparation of citrate cellulose nanocrystals

Citrate cellulose nanocrystals (Citrate CNCs) were prepared from BC using the previous method with slightly modification [19]. BC pellicles were treated in 2% NaOH solution at 90 °C for 2 h and subsequently soaked in 1% acetic acid for neutralization and rinsed with deionized water. Then, treated BC was minced by a blender (Waring commercial) for 1 min, filtered and freeze-dried. The 1 g of dried BC was treated with 6.4 g of 0.05 M HCl and 17.2 g of 80 wt% aqueous solutions of citric acid for hydrolysis and esterification of citric acid. The suspension was reflux in oil bath at 140 °C for 3 h. Consequently, the citrate CNCs slurry was severally centrifuged (14,000 rpm for 30 min) and washed until neutral pH. Finally, the citrate CNC precipitation was freeze-dried.

3.3 Characterization of citrate CNCs

3.3.1 Field emission scanning electron microscopy (FE-SEM)

The morphological examination of citrate CNCs was performed by field emission scanning electron microscopy JSM – 7610F (FE-SEM, JEOL, Tokyo, Japan) at an accelerating voltage of 5 kV mode GB high.

3.3.2 Attenuated total reflection fourier transform infrared (ATR-FTIR) spectroscopy

The ATR-FTIR spectra of BC and citrate CNCs were recorded at wavenumber range of 800 – 4000 cm^{-1} at resolution of 4 cm^{-1} using a PerkinElmer Spectrum 100 spectrophotometer. Each spectrum was obtained by averaging 16 scans.

3.3.3 Conductometric titration

The degree of substitution of citrate CNCs was evaluated by conductometer (SCHOTT,Netherland). The citrate CNCs (0.1 g) in a 0.1 M NaOH solution 2.8 mL was titrated with a 0.1 M HCl solution. Degree of substitution was calculated using the following equation (1):

$$DS = 162 \times C(V_2 - V_1) / W - (176 \times C(V_2 - V_1)) \tag{1}$$

Where V_1 = mL of HCl solution (first equivalent), V_2 = mL of HCl solution (second equivalent), C = 0.1 (molarities of HCl), W = amount of citrate CNCs used in mg, 162 = the molar mass of the AGU unit, and 176 = increase in molecular mass for the citrate CNCs.

3.3.4 X-Ray diffraction analysis (XRD)

The X-ray diffraction (XRD) patterns for BC and citrate CNCs were obtained with an X-ray diffractometer (Riggaku D/MAX-2200) using Cu target x-ray tube at 40 kV and 30 mA. Scattered radiation was detected in the range of $2\theta = 10°–40°$ at a scan rate of $5°$/min. The crystallinity index (I_C) was calculated as a function of the maximum intensity of the diffraction peak from the crystalline region (I_1), at $2\theta \sim 22.5°$ and the minimum intensity from the amorphous region (I_2), at $2\theta \sim 18°$ (Eq. (2)) [34].

$$I_C (\%) = (I_1 - I_2)/I_1 \tag{2}$$

3.3.5 Thermogravimetric analysis (TGA)

The thermogravimetric characteristic of BC and citrate CNCs were measured by TGA (SDTA851e, Mettler Toledo, Columbus, USA). This technique was used to determine the onset temperature of overall thermal degradation (T_d) of samples.

The sample was heated from 35 to 600 °C at the rate of 10 °C/min with nitrogen gas purged at 30 mL/min.

3.4 Preparation of starch/citrate CNCs nanocomposite film

Starch/citrate CNCs composite film was prepared by a solvent casting method. Three starches which were corn, wheat and rice starch were studied. Firstly, citrate CNCs suspension was prepared by dispersing the dried citrate CNCs in distilled water and sonication for 40 min. After that, starch was added and heated at 90 °C for 30 min for gelatinization. Glycerol (30 %wt of starch) was added and stirred for 10 min to obtain a homogeneous solution. After cooling down to 70 °C, the mixture was casted in polystyrene Petri dishes (14 cm diameter) and dried in an oven at 60 °C for 27 h. Dry starch film was kept in desiccator (RH = 50%) until further analysis. Four different concentrations of citrate CNCs; 5, 10, 15 and 20 %wt, were studied. Film without citrate CNCs was prepared as control film.

3.5 Characterization of films

3.5.1 Thickness

Film thickness was determined with a digital thickness gauge (SHAHE, Chengdu city, China). Each film was measured at different points at least five random locations.

3.5.2 Field emission scanning electron microscopy (FE-SEM)

The morphological examination of films was performed by field emission scanning electron microscopy JSM – 7610F (FE-SEM, JEOL, Tokyo, Japan) at an accelerating voltage of 5 kV mode GB high.

3.5.3 Attenuated total reflection fourier transform infrared (ATR-FTIR) spectroscopy

The ATR - FTIR spectra of films were recorded at wavenumber range of 800 – 4000 cm^{-1} at resolution of 4 cm^{-1} using a PerkinElmer Spectrum 100 spectrophotometer. Each spectrum was obtained by averaging 16 scans.

3.5.4 X-Ray diffraction analysis (XRD)

The X-ray diffraction (XRD) patterns for films was obtained with an X-ray diffractometer (Riggaku D/MAX-2200) using Cu target x-ray tube at 40 kV and 30 mA. Scattered radiation was detected in the range of $2\theta = 10^{\circ} - 40^{\circ}$ at a scan rate of 5°/min.

3.5.5 Thermogravimetric analysis (TGA)

The thermogravimetric characteristic of BC and citrate CNCs were measured by TGA (SDTA851e, Mettler Toledo, Columbus, USA). This technique was used to determine the onset temperature of overall thermal degradation (T_d) of samples. The sample was heated from 35 to 600 $^{\circ}$C at the rate of 10 $^{\circ}$C/min with nitrogen gas purged at 30 mL/min.

3.5.6 Differential scanning calorimetry (DSC)

Thermal transition properties of films were measured by a model Q20 differential scanning calorimeter (TA Instrument, New Castle, USA). Sample powder (about 12.0 mg) was weighted and sealed in an aluminum DSC pan. DSC scanning was performed from -130 $^{\circ}$C to 300 $^{\circ}$C at a heating rate of 10 $^{\circ}$C /min under dry nitrogen.

3.5.7 Tensile test

Films were cut into 10 × 80 mm and investigated their mechanical property (elongation at break (%ε), tensile strength (T) and Young' modulus (Y)) using universal testing machine (H10 KM) ASTM D882. A crosshead speed of 5 mm/min, gauge length of 50 mm and loaded cell of 10 KN were used. Five samples were tested in order to report as a statistical average.

3.5.8 Turbidity Light transmission and transparency

The rectangular film samples were placed directly onto the spectrophotometer cell. At selected wavelengths between 200 and 800 nm, the barrier properties of starch films against ultraviolet (UV) and visible-light transmission were measured using a UV–Vis spectrophotometer (Perkins Elmer Spectrophotometer, Korea)

according to the method described by Fang, Tung, Britt, Yada and Dalgleish [45]. Film transparency was determined by the ratio between the transmittance at 660 nm and film thickness, calculated by the following equation (3):

$$Transparency\ value = -\log T_{660}\ /\ B \tag{3}$$

Where T_{660} is the fractional transmittance at 660 nm and B is the film thickness (mm).

จุฬาลงกรณ์มหาวิทยาลัย

CHULALONGKORN UNIVERSITY

CHAPTER IV

RESULTS AND DISCUSSION

4.1 Characterization of citrate CNCs

Citrate-modified bacterial cellulose nanocrystals (citrate CNCs) were prepared by a one-pot, solvent-less, concurrent acid catalyzed reactions including hydrolysis of amorphous cellulose segments and Fischer esterification, resulting in the introduction of free carboxylic acid functionality onto CNC surfaces (Fig. 4.1).
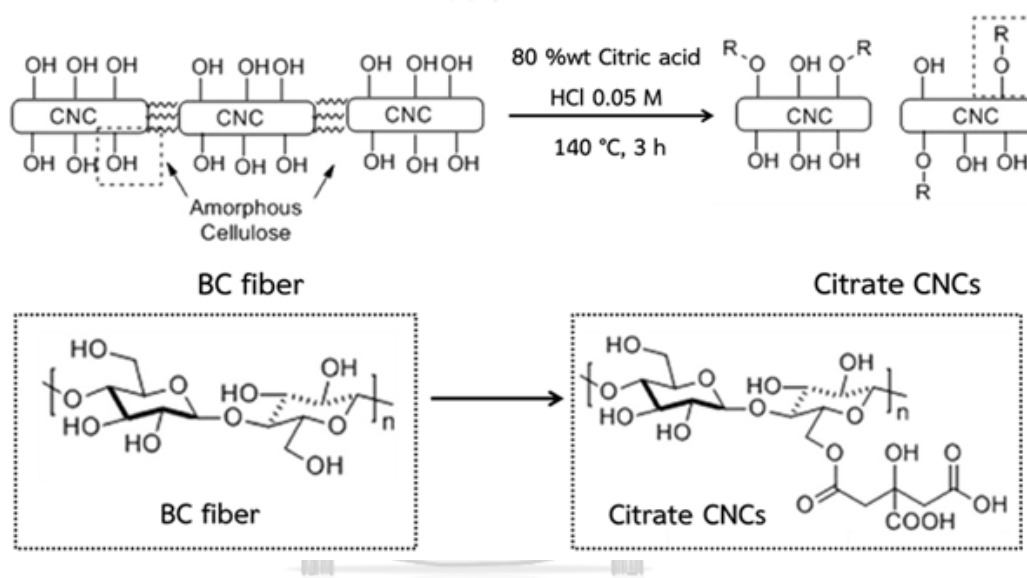

Figure 4.1 One-pot acid hydrolysis/Fischer esterification of citrate CNCs.

The morphology of BC and citrate CNCs was studied by FE-SEM (Fig. 4.2). Their length and diameters were evaluated using ImageJ software. BC had a networked structure and straight interconnected ribbon-like elements with diameter of ∼50 nm. After hydrolysis and esterification, citrate CNCs were obtained and their average lengths and widths were 583 and 46 nm, respectively. These results were different from the previous report [19], which the lengths and widths of citrate CNCs were ∼220 and ∼12 nm, respectively.
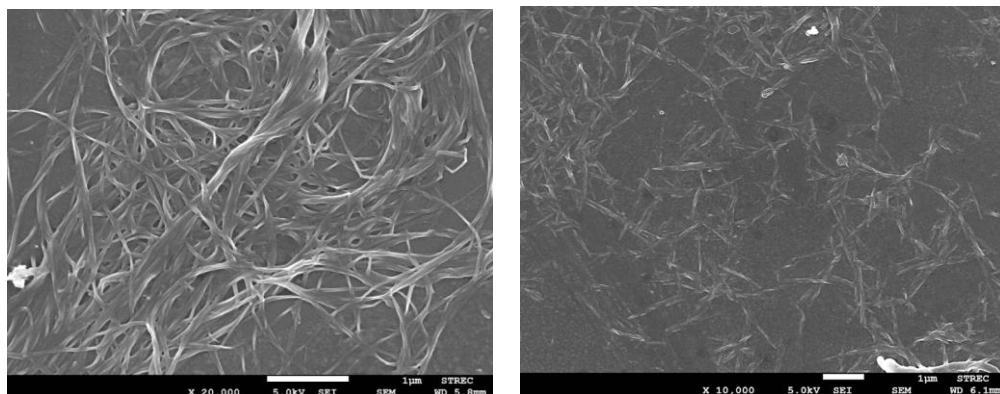
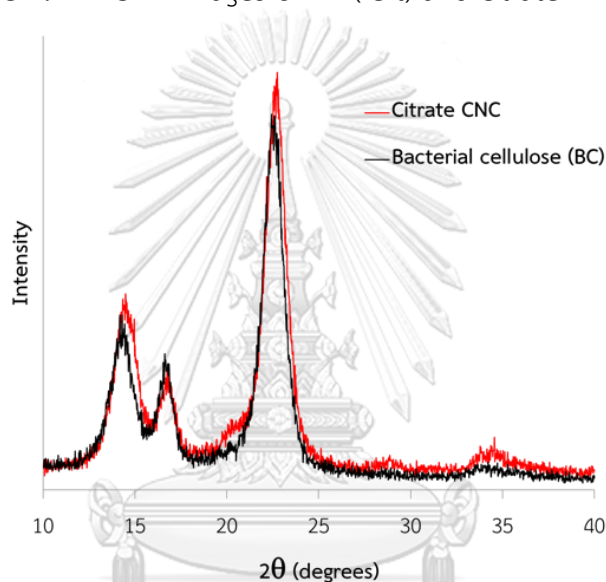**Figure 4.2** FE-SEM images of BC (left) and citrate CNCs (right)**.**

Figure 4.3 X-ray diffraction patterns of BC and citrate CNCs.

X-ray diffraction (XRD) measurements were performed on BC and citrate CNCs to observe the crystalline polymorphism. The XRD patterns were displayed in Figure 4.3. The XRD pattern of BC showed typical 2θ diffraction peaks at 14.4°, 16.7°, and 22.5° [35] whereas that of citrate CNCs showed at 14.4°, 16.7°, 22.7° and 34.5°. The crystallinity index for BC was calculated to be 90.33%, whereas that of citrate CNCs was at 93.12% closely to that of BC.

Acid functionality of citrate CNCs was evaluated by conductometric titration. Average degrees of substitution calculated from titration data were 0.075.

The functionality of citrate CNCs was investigated by FTIR. The FTIR spectra of BC and citrate CNCs (Fig. 4.4) revealed the OH stretching broad band at 3442 cm^{-1}, the C-H stretching band at 2893 cm^{-1}, the C=C stretching band at 1650 cm^{-1} and the CH$_2$ symmetric bending band at 1429 cm^{-1}. The FTIR spectra of citrate CNCs (Fig. 4.4b) showed the significant peaks at 1724 cm^{-1} that correspond to the C=O ester vibrational stretching band, which were derived from esterification between citric acid and hydroxyl groups of BC (Fig. 4.4a).

Thermal stability of BC and citrate CNCs was analyzed by TGA. The weight loss and first derivative of thermal gravity curves were shown in Figure 4.5. These data obviously showed that citrate CNCs (T$_{deg}$ = 361.9 $^\circ$C) were more thermally stable than BC (T$_{deg}$ = 357.1 $^\circ$C).
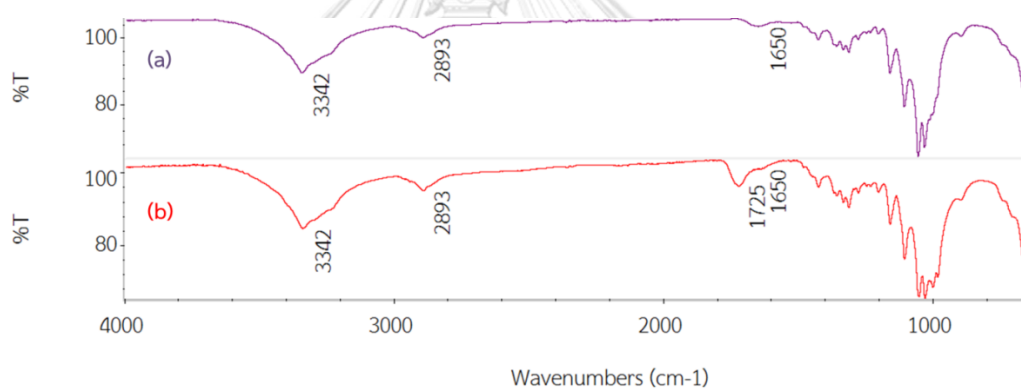

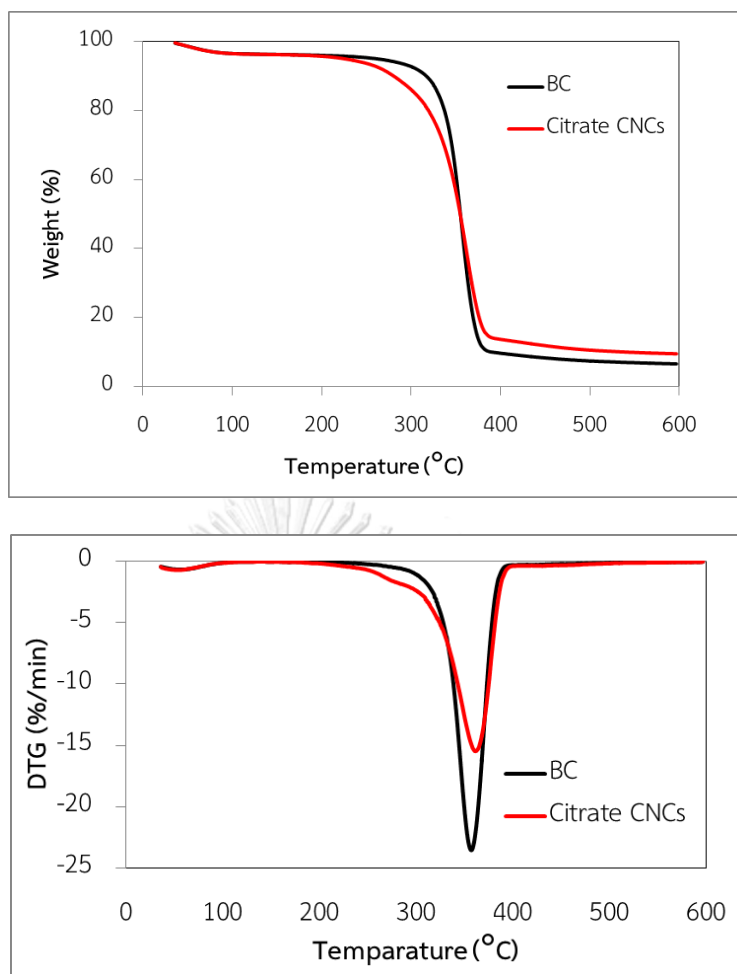**Figure 4.4** FTIR spectra of (a) BC and (b) citrate CNCs.

Figure 4.5 TG and DTG curves of BC and citrate CNCs.

Moreover, the dispersion of the citrate CNCs in the water was significant better than that of BC as showed in Figure 4.6. However, the citrate CNCs will precipitate within 10 min after sonication. The improvement of the colloidal stability was ascribed to the repulsion of negatively charged carboxylic acid functionalities presenting on the surfaces of citrate CNCs.

Figure 4.6 The dispersion of BC (left) and citrate CNCs (right) in water.

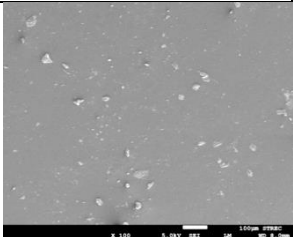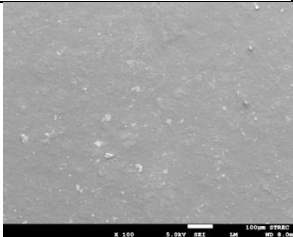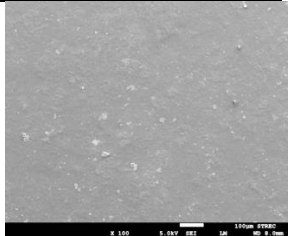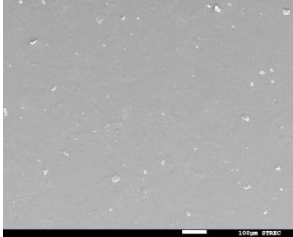## 4.2 Characterization of starch films
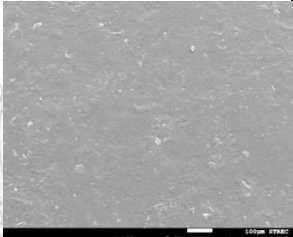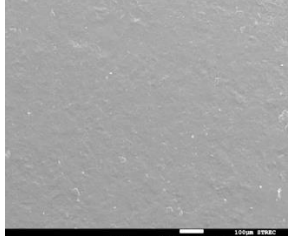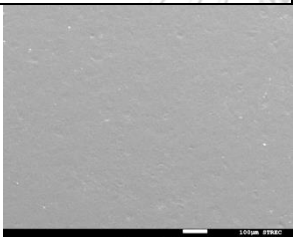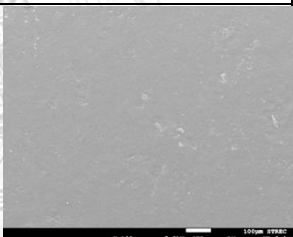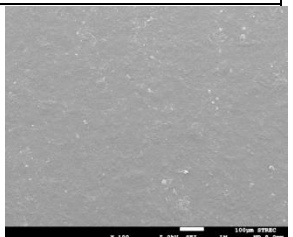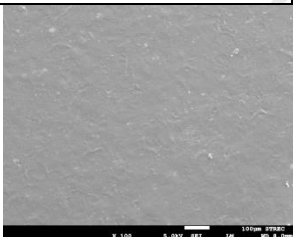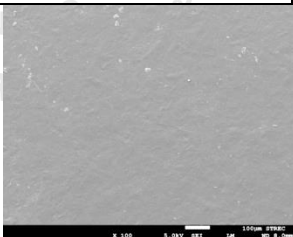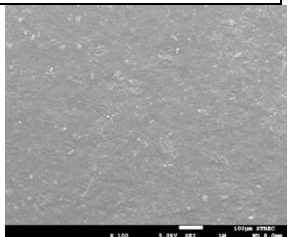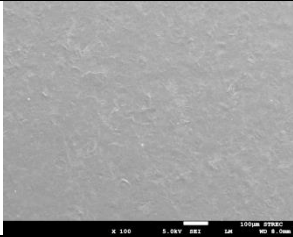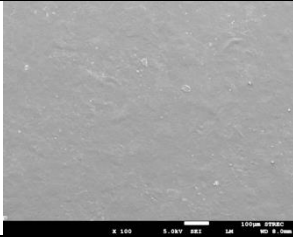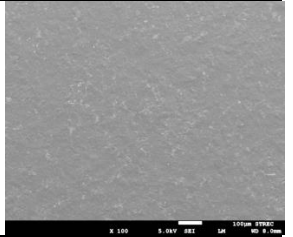
4.2.1 Morphology of starch films

Citrate CNCs (5-20 wt%) were used to reinforce the corn, wheat and rice starch films which were prepared by a casting method. The different CNCs contents were not affected the film thickness (Table 4.1). The film thickness was in a range of 0.20-0.24 mm. The surface morphology examined by SEM (Table 4.1) revealed the smooth surface with small starch aggregation for all control films. On the other hand, the rough surface with less aggregation of starch/citrate CNCs films confirmed the existence of citrate CNCs and better dispersion of film matrix. These results of corn, wheat and rice starch films gave the same appearances.

4.2.2 Attenuated total reflection fourier transform infrared (ATR-FTIR) spectroscopy

Figure 4.7 shows the FTIR spectra of starch/citrate CNCs films with different contents of citrate CNCs. The FTIR spectra of three types of starch revealed the same pattern which was the OH stretching broad band at 3281 cm^{-1}, the C-H stretching vibration band at 2926 cm^{-1}, the C=C stretching band at 1651 cm^{-1} and the C-O stretching band at 1012 and 990 cm^{-1}. The starch/citrate CNC films exhibited the same patterns of FTIR spectra as the control film. The FTIR spectra of starch/citrate CNCs films were not found the peak at 1725 cm^{-1} corresponding to the C=O ester vibrational stretching band, which were derived from citrate CNCs. Thus, this technique cannot confirm the existence of citrate CNCs in film matrix. This might be the less amount of citrate CNCs compared to starch component.

Table 4.1 FE-SEM image and thickness of starch/citrate CNCs films.

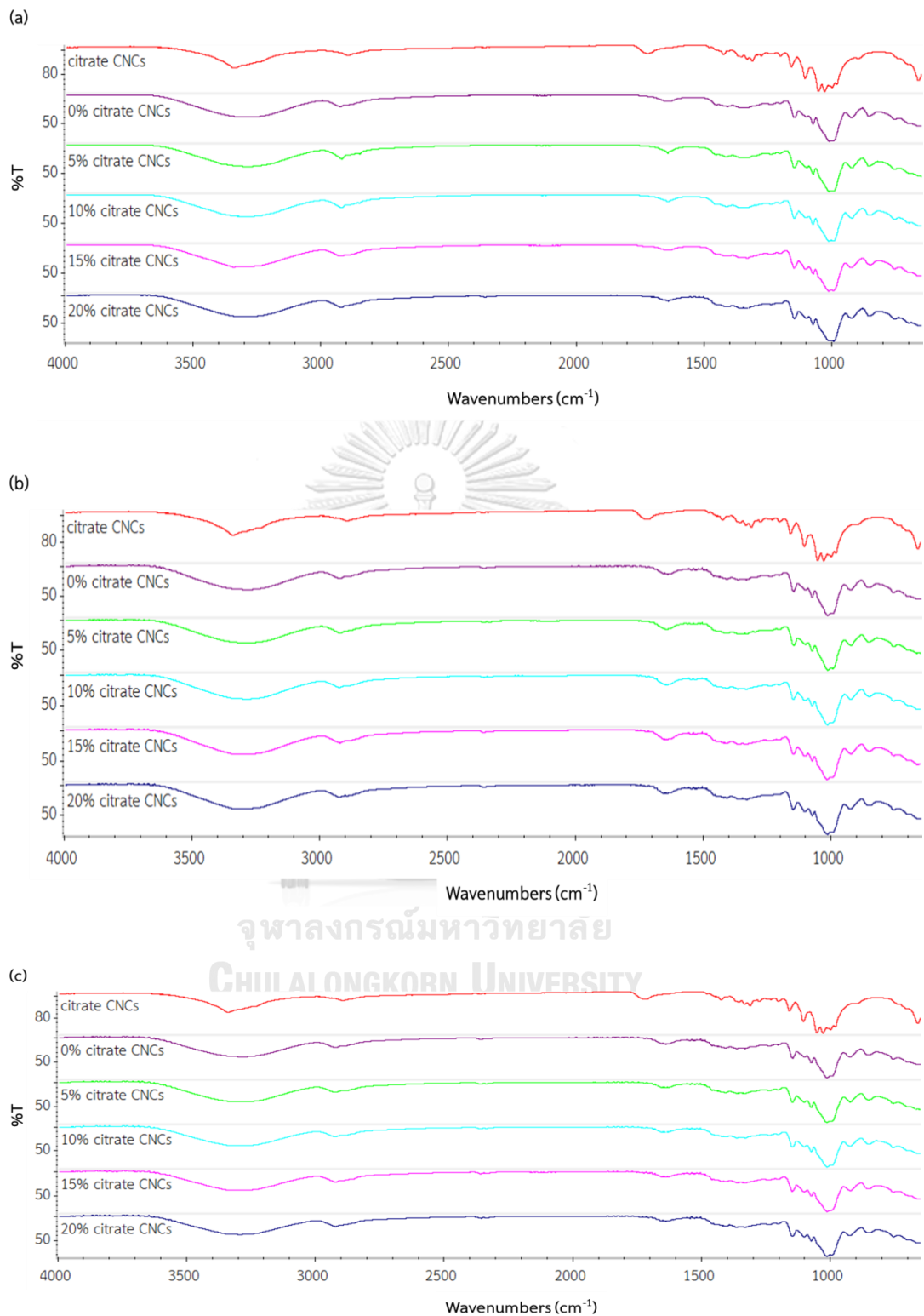| Amount of citrate CNCs	Type of starch films		
	Corn starch	Wheat starch	Rice starch
0%			
Thickness (mm)	0.22 ± 0.01	0.20 ± 0.01	0.21 ± 0.01
5%			
Thickness (mm)	0.21 ± 0.01	0.23 ± 0.01	0.22 ± 0.01
10%			
Thickness (mm)	0.21 ± 0.01	0.22 ± 0.01	0.23 ± 0.00
15%			
Thickness (mm)	0.21 ± 0.00	0.24 ± 0.01	0.24 ± 0.01
20%			
Thickness (mm)	0.23 ± 0.01	0.24 ± 0.01	0.23 ± 0.01

Figure 4.7 FTIR spectra of citrate CNCs and (a) corn, (b) wheat and (c) rice starch/citrate CNCs films.

4.2.3 X-ray diffraction analysis (XRD)

Figure 4.8 showed XRD diffraction patterns of corn, wheat and rice starch powders. Main diffraction peaks (2θ values) of all starches were almost the same which were at 15°, 17°, 18° and 23° corresponded to typical A-type crystallinity pattern [46]. Generally, amylose content of corn, wheat and rice are 27%, 25% and 20%, respectively [46]. Thus, the amylopectin content, another composition in starch, of rice starch is higher than wheat and corn starches, respectively. The crystallinity of starch is relative to the amylopectin content.

The gelatinization of starch involves both hydration and swelling of starch granules. The starch granules burst and release amylose to the outside of the granule. This causes the amylopectin to be less ordered. After cooling down, starch molecules retrograde themselves following synersis and water removal from the molecules. Thus, the crystallinity of starch decreases after gelatinization. Starch film is normally prepared by gelatinizing starch, adding plasticizer such as glycerol and drying. The addition of glycerol will decrease the crystallinity of starch film by blocking the rearrangement of starch molecules and prevented the growth of crystals on nuclei through forming strong hydrogen bonds with hydroxyl groups on starch chains [47]. These factors, gelatinization and addition of glycerol, decrease the degree of crystallinity of the starch film and give different XRD patterns comparing to starch granules.

The XRD patterns of control starch films (Fig. 4.9a) exhibited main peaks of 2θ at 17°, 19° and 22° [48] whereas those of citrate CNCs showed the strong peaks of 2θ at 14.4°, 16.7°, and 22.7°. The starch/citrate CNCs films displayed the main peaks of both starch films and citrate CNCs. An increase of the citrate CNCs content in the films enhanced the intensity of citrate CNCs peaks (Fig. 4.9c-e). No evidence of any additional peak or peak shift in the diffraction angles is observed. They showed the superimpositions of the diffractograms of the two components. This result confirmed the presence of citrate CNCs in film matrix without any interaction between two components.
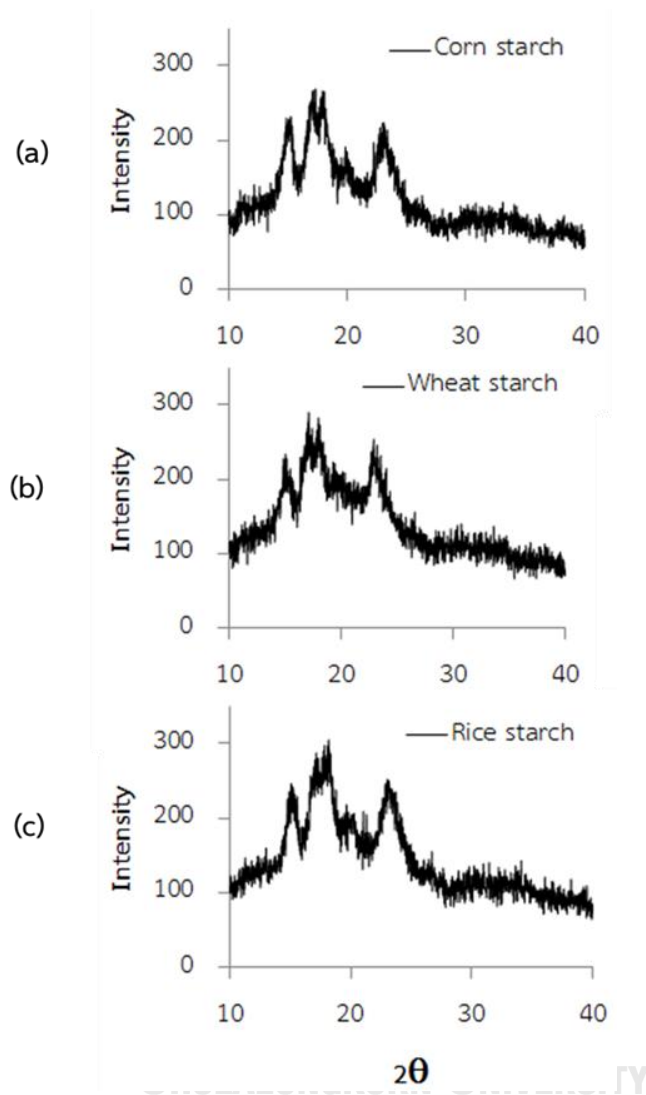
Figure 4.8 X-ray diffraction patterns of starch powders; corn, wheat and rice starch.
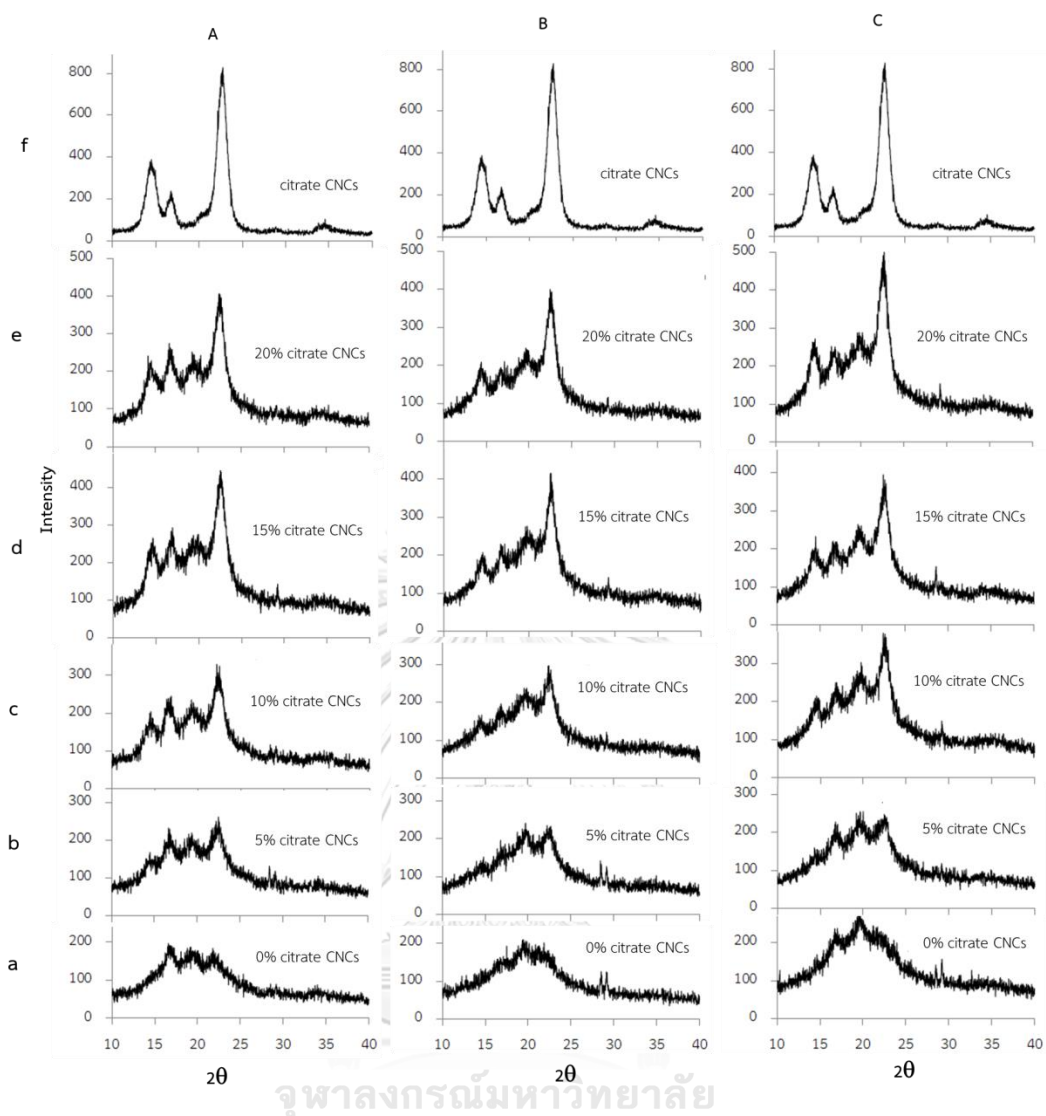
Figure 4.9 X-ray diffraction patterns of citrate CNCs and (A) corn, (B) wheat and (C) rice starch/citrate CNCs films.

4.2.4 Thermal stability

Thermogravimetric analysis was performed to evaluate the thermal stability of films. The derivative thermogravimetric (DTG) curves were shown in Fig. 4.10 and Table 2 for degradation temperature (T_{deg}) of the maximum rate of citrate CNCs, control starch films and starch/citrate CNCs films. All starch films showed T_{deg} of water and glycerol at ~100 and 200 ^{o}C, respectively. The abrupt degradation at 312-316°C and 361°C was T_{deg} of starch and citrate CNCs, respectively. The thermal stability of three starches was not insignificantly different. Thermal stability of the

starch/citrate CNCs films were appeared two main peaks of both the starch and citrate CNCs components. In addition, these results indicated that the addition of citrate CNCs showed slightly better thermal stability comparing with control starch film.

Figure 4.11 represented the Differential scanning calorimetry (DSC) thermograms of citrate CNCs, control starch films and starch/citrate CNCs films. The melting temperature (T_m) of them was presented in Table 2. The T_m of citrate CNCs was 84.8°C which was lower than those of three starches. The addition of citrate CNCs decreased the melting point of the starch films. At the highest content of citrate CNCs (20%wt), the T_m of rice, corn and wheat starch/citrate CNC films decreased 14.7, 6.5 and 4.6 percentages comparing to those of control starch films, respectively. These result ascribed to the good dispersion and interfacial adhesion of citrate CNCs, which hindered the horizontal reorganization of starch molecular chains and the crystallization effect of amylopectin molecules [44].As a result, the melting point of the starch/citrate CNCs film was decreased to some extent.

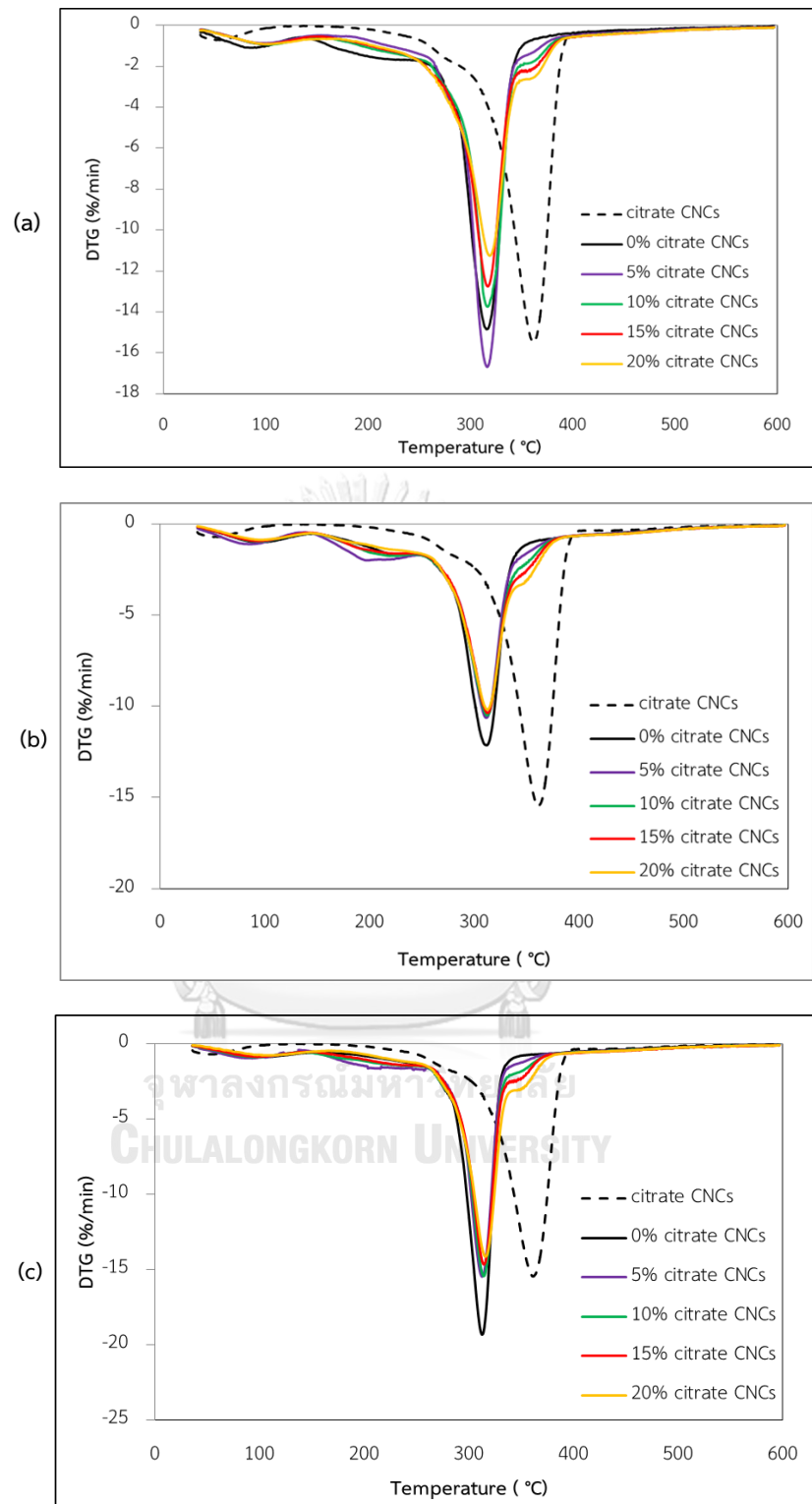**Figure 4.10** DTG curves of citrate CNCs and (a) corn, (b) wheat and (c) rice starches/citrate CNCs films.
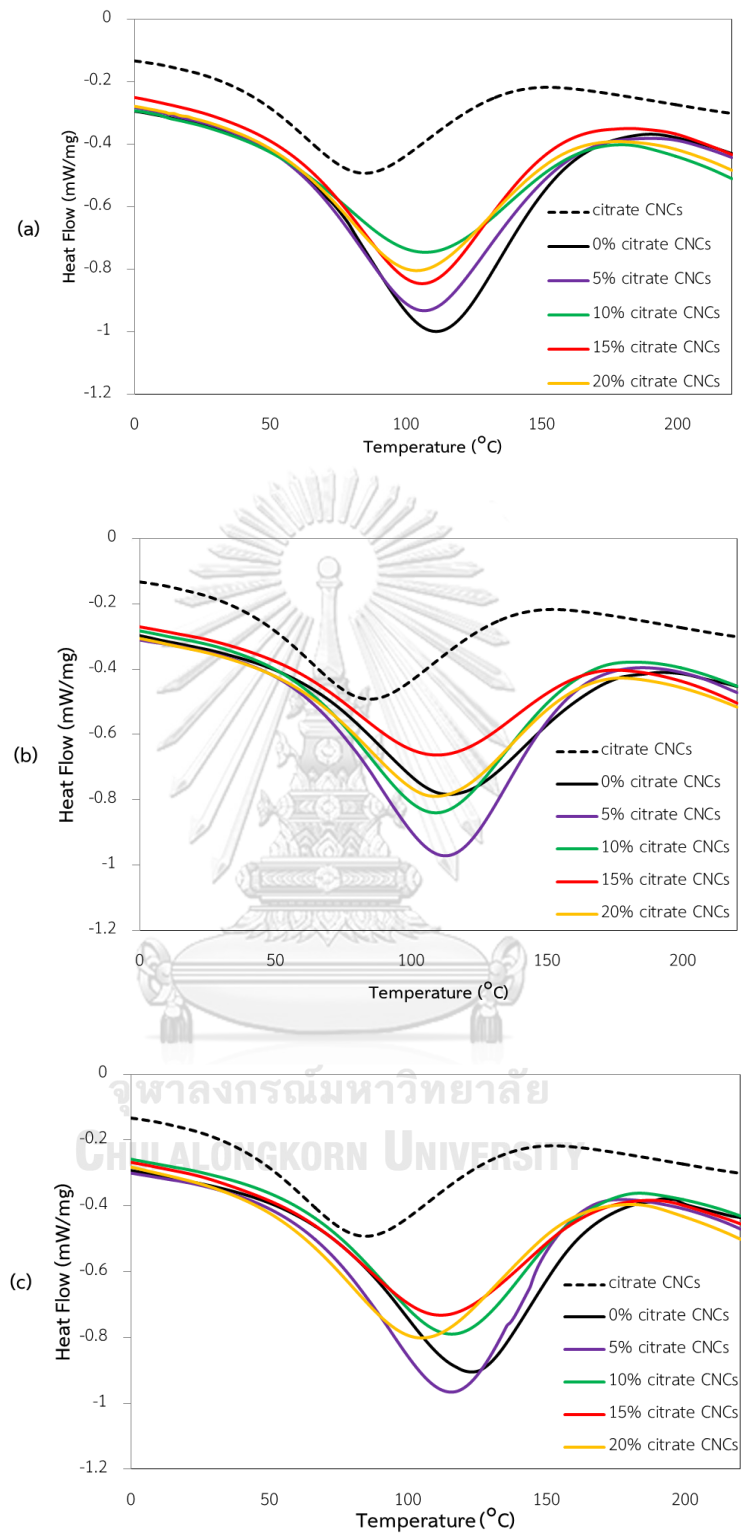
Figure 4.11 DSC curves of citrate CNCs and (a) corn, (b) wheat and (c) rice starches/citrate CNCs films.

Table 4.2 TGA and DSC results.

Sample	% citrate CNCs	Degradation temperature (max DTG peak) (^{o}C)	T_m (^{o}C)
Citrate CNCs	-	361.9	84.8
Corn starch film	0	315.7	111.1
	5	316.2	106.7
	10	316.8	107.1
	15	317.1	105.9
	20	319.1	103.8
Wheat starch film	0	311.7	114.2
	5	312.0	112.6
	10	312.8	109.5
	15	313.2	109.1
	20	313.3	108.9
Rice starch film	0	312.6	123.0
	5	312.9	115.8
	10	314.3	115.6
	15	314.6	111.9
	20	316.0	104.9

4.2.5 Mechanical property

The tensile strength and Young's modulus of the corn, wheat and rice starch films and reinforced with various contents of citrate CNCs were presented in Figure 4.12 and Table 4.3. Different type of starch had different the mechanical properties. Corn starch film had higher tensile strength and Young's modulus values than rice and wheat starch films, respectively.

The addition of citrate CNCs has effect on the mechanical properties of three starch films in the same trend. At 5%wt citrate CNCs, the mechanical property of composite films had not different comparing to control films. When the citrate CNCs

content increased to more than 5%wt, the mechanical property gradually increased except for rice starch/citrate CNCs films. Both tensile strength and Young's modulus of the rice starch film with 20%wt citrate CNCs dramatically enhanced. The rigid network in the starch/citrate CNCs film can probably be explained by the reinforcement effect from good dispersed of citrate CNCs fillers in the starch matrix and the strong hydrogen bonding between interfaces of citrate CNC and starch.
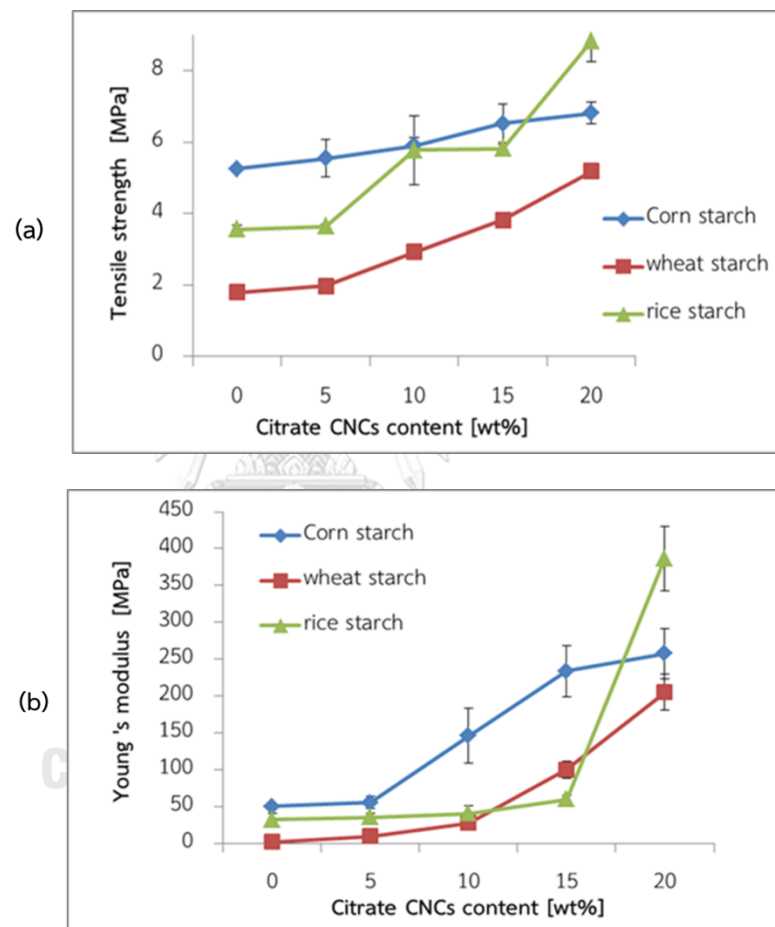

Figure 4.12 The tensile strength (a) and Young's modulus (b) of corn, wheat and rice starches films as a function of citrate CNCs content

Table 4.3 Mechanical properties of corn, wheat and rice starch/citrate CNCs films.

Starch film	% citrate CNCs	Tensile strength [MPa]	Young 's modulus [MPa]
Corn	0	5.26 ± 0.01	50.64 ± 2.19
	5	5.55 ± 0.53	55.82 ± 8.36
	10	5.91 ± 0.21	146.32 ± 37.30
	15	6.53 ± 0.53	234.00 ± 34.46
	20	6.82 ± 0.31	257.60 ± 34.37
Wheat	0	1.79 ± 0.14	2.48 ± 0.23
	5	1.98 ± 0.05	10.13 ± 1.23
	10	2.93 ± 0.21	27.75 ± 6.62
	15	3.82 ± 0.09	100.28 ± 11.72
	20	5.19 ± 0.22	204.90 ± 24.31
Rice	0	3.56 ± 0.13	32.49 ± 8.06
	5	3.64 ± 0.07	35.57 ± 5.57
	10	5.78 ± 0.96	40.50 ± 10.99
	15	5.82 ± 0.11	60.22 ± 5.35
	20	8.84 ± 0.58	386.50 ± 43.88

4.2.6 Transparency

Figure 4.13 shows the transparency value of control starch films; corn, wheat and rice starches and starch films contained various content of citrate CNCs. The higher value represents the lower transparence of the films. The result showed that rice starch had higher transparency values, followed by wheat and corn starch, respectively. The addition of citrate CNCs affected the increasing transparency values or turbidity of films. The photograph images of films showed in Figure 4.14.
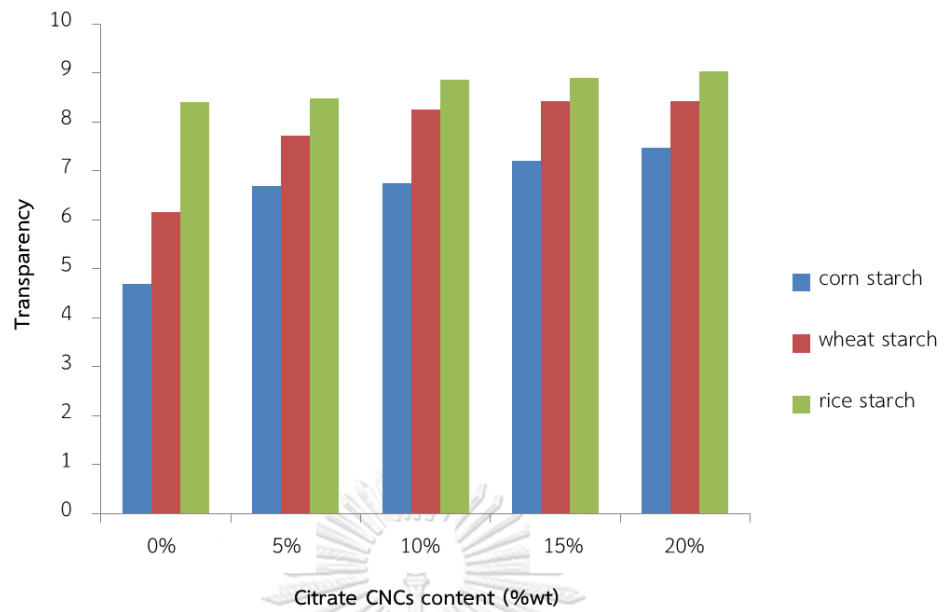
Figure 4.13 Transparency of corn, wheat and rice starches films as a function of citrate CNCs content.
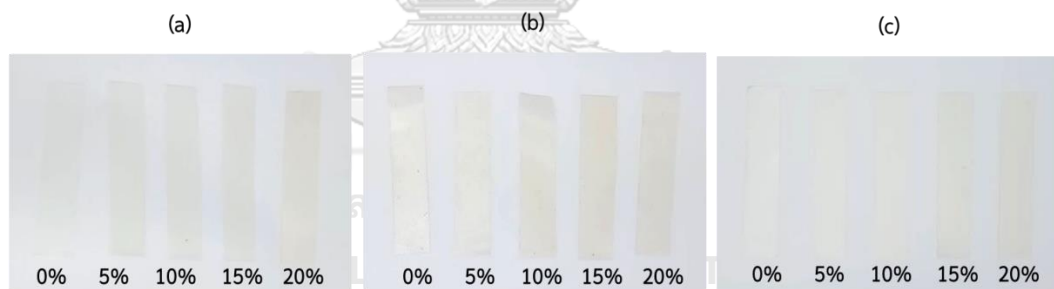

Figure 4.14 Corn (a), wheat (b) and rice (c) starch films with various citrate CNCs content.

CHAPTER V

CONCLUSION

This study reported the preparation of citrate-modified bacterial cellulose nanocrystals (citrate CNCs) by a green one-pot dual acid (citric and hydrochloric acids) method and used them to reinforce three types of starch films; corn, wheat and rice starch films. The degree of carboxyl group substitution on CNCs was 0.075. The average length and width of citrate CNCs were 583 and 46 nm, respectively. The crystallinity index for citrate CNCs was closely to the original BC.

Starch films containing various amount of citrate CNCs were prepared by a solvent casting method. The film thickness of most films was in a range of 0.20-0.24 mm. The SEM images revealed the good dispersion of citrate CNCs in the film matrix. Physical property of control films and starch-20%citrate CNCs films were summarized in Table 5.1. The addition of citrate CNCs in all starches showed the continuing enhancement of crystallinity, degradation temperature, mechnical property and transparency, except for T_m. The tensile strength of starch/citrate CNCs films increased gradually while Young's modulus increased dramatically. This indicated that the elasticity of films decreased if the amount of citrate CNCs increased. Among of three starches, wheat stach films had the most effect from incorpartion of citrate CNCs

Table 5.1 Summary data of physical property of control and starch/20%wt citrate CNCs.

	Corn starch film			Wheat starch film			Rice starch film		
	control	20%[a]	% increase[b]	control	20%[a]	% increase[b]	control	20%[a]	% increase[b]
Crystallinity			-			-			-
T_{deg}	315.7	319.1	1.07	311.7	313.3	0.51	312.6	316.0	1.08
T_m	111.1	103.8	-	114.2	108.9	-	123.0	104.9	-
Tensile strength	5.3	6.8	29.6	1.8	5.2	189.9	3.6	8.8	148.3
Young's modulus	50.7	257.6	0.4×10^3	2.5	204.9	8.2×10^3	32.5	386.5	1.1×10^3
Transparancy	4.7	7.5	59.1	6.2	8.4	36.9	8.4	9.0	7.5

a: the property value of strach-20%wt citrate CNCs film

b: increasing percentages of the of strach-20%wt citrate CNCs film compared to control film

REFERENCES

[1]   Smith, A.M. The biosynthesis of starch granules. Biomacromolecules 2 (2001): 335-341.

[2]   Wittaya, T. Rice starch-based biodegradable films: properties enhancement. in Structure and function of food engineering: InTech, 2012.

[3]   Cheetham, N.W. and Tao, L. Variation in crystalline type with amylose content in maize starch granules: an X-ray powder diffraction study. Carbohydrate polymers 36 (1998): 277-284.

[4]   Mali, S., Grossmann, M.V.E., García, M.A., Martino, M.N., and Zaritzky, N.E. Barrier, mechanical and optical properties of plasticized yam starch films. Carbohydrate Polymers 56 (2004): 129-135.

[5]   De Carvalho, A., Curvelo, A., and Agnelli, J. A first insight on composites of thermoplastic starch and kaolin. Carbohydrate Polymers 45 (2001): 189-194.

[6]   Dai, L., Qiu, C., Xiong, L., and Sun, Q. Characterisation of corn starch-based films reinforced with taro starch nanoparticles. Food chemistry 174 (2015): 82-88.

[7]   Cao, X., Chen, Y., Chang, P.R., and Huneault, M.A. Preparation and properties of plasticized starch/multiwalled carbon nanotubes composites. Journal of Applied Polymer Science 106 (2007): 1431-1437.

[8]   Lepifre, S., et al. Lignin incorporation combined with electron-beam irradiation improves the surface water resistance of starch films. Biomacromolecules 5 (2004): 1678-1686.

[9]   Dias, A.B., Müller, C.M., Larotonda, F.D., and Laurindo, J.B. Mechanical and barrier properties of composite films based on rice flour and cellulose fibers. LWT-Food Science Technology 44 (2011): 535-542.

[10]   Cao, X., Chen, Y., Chang, P., Muir, A., and Falk, G. Starch-based nanocomposites reinforced with flax cellulose nanocrystals. Express Polymer Letters 2 (2008): 502-510.

[11]   Eichhorn, S.J., et al. current international research into cellulose nanofibres and nanocomposites. Journal of materials science 45 (2010): 1.

[12]   Anwar, B., Rosyid, N.H., Effendi, D.B., Nandiyanto, A.B.D., Mudzakir, A., and Hidayat, T. Isolation of bacterial cellulose nanocrystalline from pineapple peel waste: Optimization of acid concentration in the hydrolysis method. in AIP Conference Proceedings, p. 040001: AIP Publishing, 2016.

[13]   Reiniati, I., Hrymak, A.N., and Margaritis, A. Recent developments in the production and applications of bacterial cellulose fibers and nanocrystals. Critical reviews in biotechnology 37 (2017): 510-524.

[14]   Wan, Y., Luo, H., He, F., Liang, H., Huang, Y., and Li, X. Mechanical, moisture absorption, and biodegradation behaviours of bacterial cellulose fibre-reinforced starch biocomposites. Composites Science Technology 69 (2009): 1212-1217.

[15]   Quero, F., et al. Optimization of the mechanical performance of bacterial cellulose/poly (L-lactic) acid composites. ACS applied materials 2 (2009): 321-330.

[16]   Gea, S., Bilotti, E., Reynolds, C., Soykeabkeaw, N., and Peijs, T. Bacterial cellulose–poly (vinyl alcohol) nanocomposites prepared by an in-situ process. Materials Letters 64 (2010): 901-904.

[17]   Phomrak, S. and Phisalaphong, M. Reinforcement of natural rubber with bacterial cellulose via a latex aqueous microdispersion process. Journal of Nanomaterials 2017 (2017).

[18]   Pinto, E., et al. Transparent composites prepared from bacterial cellulose and castor oil based polyurethane as substrates for flexible OLEDs. Journal of Materials Chemistry C 3 (2015): 11581-11588.

[19]   Spinella, S., et al. Concurrent cellulose hydrolysis and esterification to prepare a surface-modified cellulose nanocrystal decorated with carboxylic acid moieties. ACS Sustainable Chemistry 4 (2016): 1538-1550.

[20]   Braun, B. and Dorgan, J.R. Single-step method for the isolation and surface functionalization of cellulosic nanowhiskers. Biomacromolecules 10 (2008): 334-341.

[21]   Spinella, S., et al. Polylactide/cellulose nanocrystal nanocomposites: Efficient routes for nanofiber modification and effects of nanofiber chemistry on PLA reinforcement. Polymer 65 (2015): 9-17.

[22]   Tokoh, C., Takabe, K., Fujita, M., and Saiki, H. Cellulose synthesized by Acetobacter xylinum in the presence of acetyl glucomannan. <u>Cellulose</u> 5 (1998): 249-261.

[23]   Klemm, D., et al. Nanocelluloses: a new family of nature-based materials. <u>Angewandte Chemie International Edition</u> 50 (2011): 5438-5466.

[24]   Son, H.-J., Kim, H.-G., Kim, K.-K., Kim, H.-S., Kim, Y.-G., and Lee, S.-J. Increased production of bacterial cellulose by Acetobacter sp. V6 in synthetic media under shaking culture conditions. <u>Bioresource Technology</u> 86 (2003): 215-219.

[25]   Klemm, D., Heublein, B., Fink, H.P., and Bohn, A. Cellulose: fascinating biopolymer and sustainable raw material. <u>Angewandte Chemie International Edition</u> 44 (2005): 3358-3393.

[26]   Klemm, D. <u>Polysaccharides II</u>. Vol. 205: Springer, 2006.

[27]   Torgbo, S. and Sukyai, P. Bacterial cellulose-based scaffold materials for bone tissue engineering. <u>Applied Materials Today</u> 11 (2018): 34-49.

[28]   Kucińska-Lipka, J., Gubanska, I., and Janik, H. Bacterial cellulose in the field of wound healing and regenerative medicine of skin: recent trends and future prospectives. <u>Polymer Bulletin</u> 72 (2015): 2399-2419.

[29]   Hu, W., Chen, S., Yang, J., Li, Z., and Wang, H. Functionalized bacterial cellulose derivatives and nanocomposites. <u>Carbohydrate polymers</u> 101 (2014): 1043-1060.

[30]   Choi, Y.J., Ahn, Y., Kang, M.S., Jun, H.K., Kim, I.S., and Moon, S.H. Preparation and characterization of acrylic acid-treated bacterial cellulose cation-exchange membrane. <u>Journal of Chemical Technology Biotechnology: International Research in Process, Environmental Clean Technology</u> 79 (2004): 79-84.

[31]   Shah, J., Malcolm Brown, R., and Biotechnology. Towards electronic paper displays made from microbial cellulose. <u>Applied Microbiology</u> 66 (2005): 352-355.

[32]   Trovatti, E., et al. Novel bacterial cellulose–acrylic resin nanocomposites. <u>Composites Science and Technology</u> 70 (2010): 1148-1153.

[33]   Phomrak, S. and Phisalaphong, M. Reinforcement of Natural Rubber with Bacterial Cellulose via a Latex Aqueous Microdispersion Process <u>Journal of</u>

Nanomaterials 2017 (2017): 9.

[34]   Vasconcelos, N.F., et al. Bacterial cellulose nanocrystals produced under different hydrolysis conditions: Properties and morphological features. Carbohydrate Polymers 155 (2017): 425-431.

[35]   Martínez-Sanz, M., Lopez-Rubio, A., and Lagaron, J.M. Optimization of the nanofabrication by acid hydrolysis of bacterial cellulose nanowhiskers. Carbohydrate Polymers 85 (2011): 228-236.

[36]   George, J. and Siddaramaiah. High performance edible nanocomposite films containing bacterial cellulose nanocrystals. Carbohydrate Polymers 87 (2012): 2031-2037.

[37]   Han, G., Huan, S., Han, J., Zhang, Z., and Wu, Q. Effect of Acid Hydrolysis Conditions on the Properties of Cellulose Nanoparticle-Reinforced Polymethylmethacrylate Composites. Materials 7 (2014).

[38]   Lin, N., Huang, J., Chang, P.R., Feng, J., and Yu, J. Surface acetylation of cellulose nanocrystal and its reinforcing function in poly(lactic acid). Carbohydrate Polymers 83 (2011): 1834-1842.

[39]   Abou-Zeid, R.E., Hassan, E.A., Bettaieb, F., Khiari, R., and Hassan, M.L. Use of cellulose and oxidized cellulose nanocrystals from olive stones in chitosan bionanocomposites Journal of Nanomaterials 2015 (2015): 11.

[40]   Ferreira, F.V., Mariano, M., Rabelo, S.C., Gouveia, R.F., and Lona, L.M.F. Isolation and surface modification of cellulose nanocrystals from sugarcane bagasse waste: From a micro- to a nano-scale view. Applied Surface Science 436 (2018): 1113-1122.

[41]   Jiménez, A., Fabra, M.J., Talens, P., and Chiralt, A. Edible and Biodegradable Starch Films: A Review. Food Bioprocess Technology 5 (2012): 2058-2076.

[42]   Carvalho, A.J.F. Properties and Applications as Thermoplastic Materials. in Belgacem, M.N. and Gandini, A. (eds.),Monomers, Polymers and Composites from Renewable Resources, pp. 321-342. Amsterdam: Elsevier, 2008.

[43]   Slavutsky, A.M. and Bertuzzi, M.A. Water barrier properties of starch films reinforced with cellulose nanocrystals obtained from sugarcane bagasse.

Carbohydrate Polymers 110 (2014): 53-61.

[44]   Ma, X., Cheng, Y., Qin, X., Guo, T., Deng, J., and Liu, X. Hydrophilic modification of cellulose nanocrystals improves the physicochemical properties of cassava starch-based nanocomposite films. LWT-Food Science Technology 86 (2017): 318-326.

[45]   Chentir, I., et al. Biofunctional gelatin-based films incorporated with food grade phycocyanin extracted from the Saharian cyanobacterium Arthrospira sp. Food Hydrocolloids (2018).

[46]   Alcázar-Alay, S.C. and Meireles, M.A.A. Physicochemical properties, modifications and applications of starches from different botanical sources. Journal of Food Science Technology 35 (2015): 215-236.

[47]   Farahnaky, A., Saberi, B., and Majzoobi, M. Effect of glycerol on physical and mechanical properties of wheat starch edible films. Journal of Texture Studies 44 (2013): 176-186.

[48]   Cui, S., Li, M., Zhang, S., Liu, J., Sun, Q., and Xiong, L. Physicochemical properties of maize and sweet potato starches in the presence of cellulose nanocrystals. Food Hydrocolloids 77 (2018): 220-227.

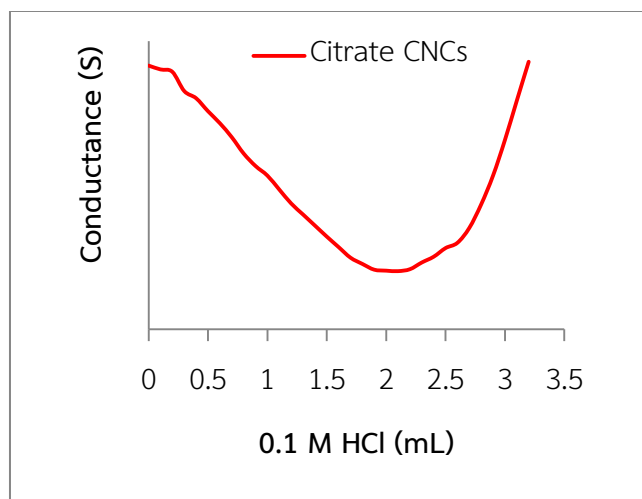APPENDIX

Appendix A

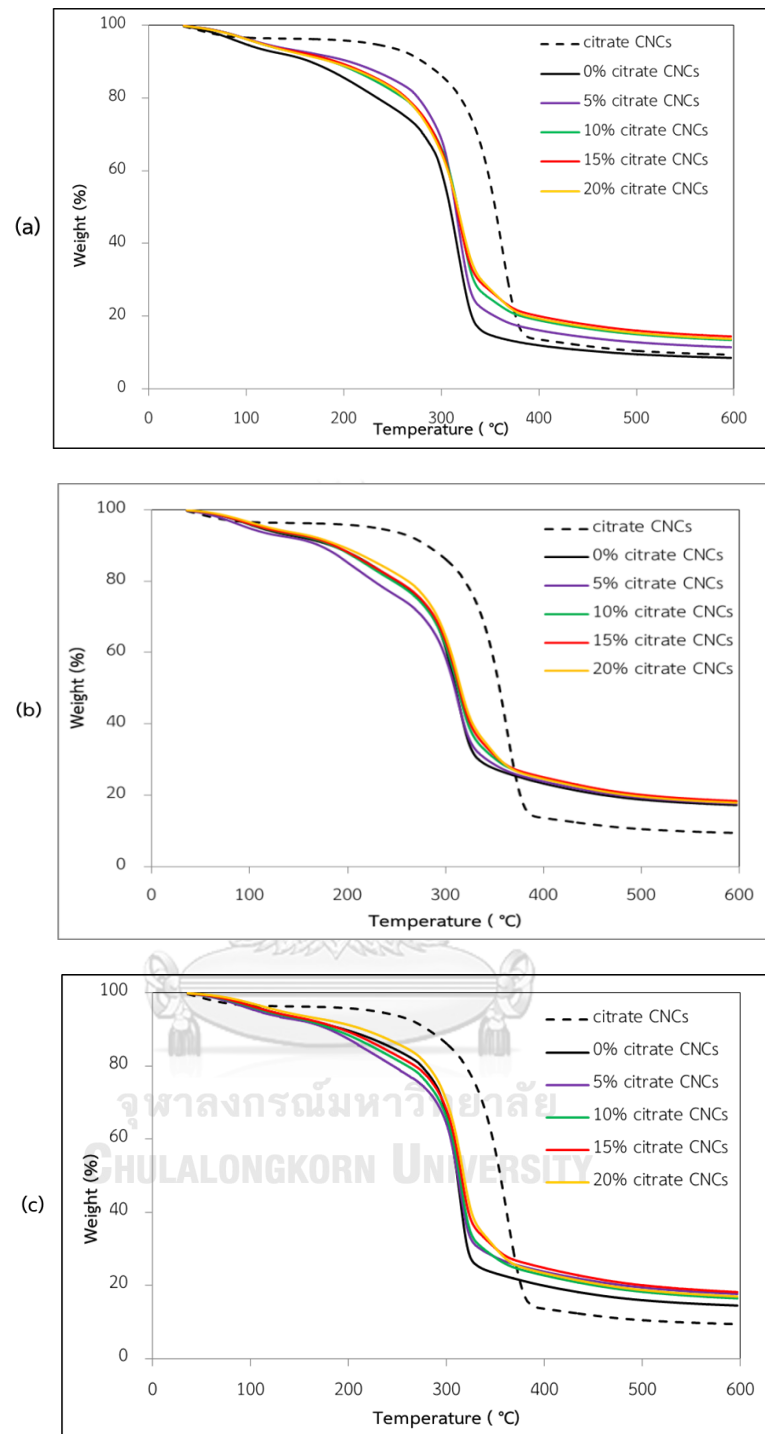**Figure A1** Conductometric titration of citrate CNCs with 0.1 M HCl.

Figure A2 TG curves of citrate CNCs and (a) corn, (b) wheat and (c) rice

starches/citrate CNCs films.

Table A1 Transparency values of corn, wheat and rice starches films as a function of citrate CNCs content.

Starch film	% citrate CNCs content	Transparency value
corn	0	4.69
	5	6.68
	10	6.75
	15	7.20
	20	7.47
wheat	0	6.16
	5	7.72
	10	8.26
	15	8.42
	20	8.43
rice	0	8.40
	5	8.48
	10	8.85
	15	8.89
	20	9.02

VITA

NAME	Miss Prapaporn Nakarat
DATE OF BIRTH	01 December
PLACE OF BIRTH	Nakhonratchasima
INSTITUTIONS ATTENDED	Bachelor's Degree from Department of Chemistry, Faculty of science, Thammasat University, 2011-2015. Master' s Degree from Program in Petrochemistry and polymer science, Faculty of science, Chulalongkorn University.
HOME ADDRESS	161, Moo.6, Lummoon, Noonsung , Nakhonratchasima, 30160
PUBLICATION	Poster presentation "Corn starch film reinforced with citrate cellulose nanocrystals" at the 44th Congress on Science and Technology of Thailand "Science and Technology in the Disruptive Era", Bangkok International Trade & Exhibition Centre (BITEC), Bangkok, Thailand, 29 – 31 October 2018

จุฬาลงกรณ์มหาวิทยาลัย
CHULALONGKORN UNIVERSITY